AER/AGS Report 98

Hydrogeological Characterization of the Upper Cretaceous–Quaternary Units in the Fox Creek Area, West-Central Alberta

AER/AGS Report 98

Hydrogeological Characterization of the Upper Cretaceous–Quaternary Units in the Fox Creek Area, West-Central Alberta

B.D. Smerdon[1], J. Klassen[1] and W.P Gardner[2]

[1] Alberta Energy Regulator
Alberta Geological Survey
[2] Department of Geosciences, University of Montana

September 2019

ISBN 978-1-4601-4496-1

Smerdon, B.D., Klassen, J. and Gardner, W.P. (2019): Hydrogeological characterization of the Upper Cretaceous–Quaternary units in the Fox Creek area, west-central Alberta; Alberta Energy Regulator / Alberta Geological Survey, AER/AGS Report 98, 35 p.

Author addresses:
W.P. Gardner
Department of Geosciences
University of Montana
Missoula, MT 59812-1296
U.S.
Tel: 406.243.2458
Email: payton.gardner@umontana.edu

Published September 2019 by:
Alberta Energy Regulator
Alberta Geological Survey
4th Floor, Twin Atria Building
4999 – 98th Avenue
Edmonton, AB T6B 2X3
Canada

Tel: 780.638.4491
Fax: 780.422.1459
Email: AGS-Info@aer.ca
Website: www.ags.aer.ca

Contents

Tables

Figures

Acknowledgements

The authors wish to acknowledge the following individuals for their contributions to this report:

- S. Stewart (AGS) for her assistance with the Alberta Water Well Information Database and compiling groundwater chemistry data,
- A. Hughes (AGS summer student) for developing the potentiometric surface and her work on hydraulic properties of the Paskapoo Formation,
- N. Nakevska (AGS) for her assistance with fieldwork in the fall of 2015, and
- L.D. Andriashek (AGS) for his continued discussions about groundwater in the uppermost bedrock of the study area and providing a science review of this report.

Abstract

The hydrogeological characteristics and interaction with surface water are described for an area surrounding the Town of Fox Creek, west-central Alberta. Hydrogeological mapping and water samples acquired as part of this study were used to develop a conceptual understanding of groundwater circulation. Key attributes of the geological framework were used to map regional hydraulic pathways.

Groundwater recharge is expected to be enhanced in the area southwest of Fox Creek, compared to other parts of the study area. Similarly, groundwater movement in the bedrock is aided by abundant sandstone in the uppermost part of the Paskapoo Formation southwest of Fox Creek. The potentiometric surface reflects ground surface topography with groundwater flowing from the benchlands in the southwestern margin of the study area and the Swan Hills in the northeast, towards the north. The exception is the southeastern margin of the study area where groundwater flow is towards the Athabasca River. Concentrations of naturally occurring environmental tracers indicated that the rivers contain water with a mean age of less than a decade. Analysis of downstream trends in river water sample results found that rivers only received an appreciable amount of baseflow where they were in close proximity to bedrock with high sandstone abundance. The rivers generally had decreasing baseflow as the underlying bedrock formations transitioned from the Paskapoo Formation to the Scollard and Wapiti formations to the north.

The hydrogeological characteristics of this region are summarized by two conceptual hydrogeological landscapes that are based on topographic relief. Where sandstone is abundant in the subsurface, relief is high, resulting in deeper groundwater circulation and older baseflow sources to rivers. Relief is low in areas of less-resistant bedrock and surface sediments, which generally have lower hydraulic conductivity, thereby limiting groundwater recharge and resulting in more localized groundwater capture to rivers with younger baseflow sources.

1 Introduction

The west-central part of Alberta, including the upper sections of the Peace River and Athabasca River drainage basins, encompasses the significant shale gas plays of the Montney and Duvernay formations, an active forestry industry, and headwaters of many tributaries that drain into the Peace and Athabasca rivers. The effects of development occurring from the co-location of different industries in this region will increase pressure on land and water resources. Managing natural resources through a regional planning process will rely in part on understanding the hydrogeological framework of this region and the circulation of groundwater. The demand for water to support energy development has increased in west-central Alberta, especially in the region surrounding the Town of Fox Creek (Alberta Energy Regulator, 2019). In the early stages of development, water has routinely been sourced from surface water and shallow groundwater for activities such as hydraulic fracturing. However, knowledge of these nonsaline hydrological systems is generally lacking, and understanding and managing the cumulative effects of water use requires defensible geoscience.

The objective of this study is to characterize the regional hydrogeology in the Fox Creek area (Figure 1) in order to advance the knowledge of nonsaline groundwater circulation and interaction with surface water, and to establish groundwater conditions to support regulation decisions and assessment of cumulative effects. The study achieved the following:

- a description of the hydrostratigraphic framework, with an emphasis on how specific units contribute to the pattern of groundwater movement and interaction with surface water;
- maps of the distribution of water level and water chemistry data to understand the potentiometric surface and total dissolved solids (TDS) of groundwater within the uppermost bedrock units in the region;
- estimates of the regional recharge and discharge areas, including analysis of vertical gradients and delineating the sources of baseflow to three river systems in the region (Little Smoky River, Deep Valley Creek–Simonette river system, Wildhay–Berland river system).

This study is part of a suite of geoscience products published by the Alberta Geological Survey (AGS) focusing on west-central Alberta, including

- field evidence of nested groundwater flow along the Little Smoky River, west-central Alberta (AER/AGS Open File Report 2016-02 [Smerdon et al., 2016]),
- summary of hydraulic conductivity values for the Paskapoo Formation in west-central Alberta (AER/AGS Open File Report 2016-03 [Hughes et al., 2017b]),
- three-dimensional (3D) rendering of the regional stratigraphy of Paleogene–Quaternary sediments in west-central Alberta (AER/AGS Report 93 [Atkinson and Hartman, 2017]),
- regional stratigraphic correlation and 3D geological modelling of west-central Alberta (AER/AGS Open File Report 2019-04 [Corlett et al., 2019]),
- west-central Alberta 3D geological model – methodology and metadata (AER/AGS Model 2019-03 [Babakhani and MacCormack, 2019]),
- 3D property modelling of the bedrock hydrostratigraphy in the Fox Creek area, west-central Alberta (AER/AGS Open File Report 2019-03 [Babakhani et al., 2019]).

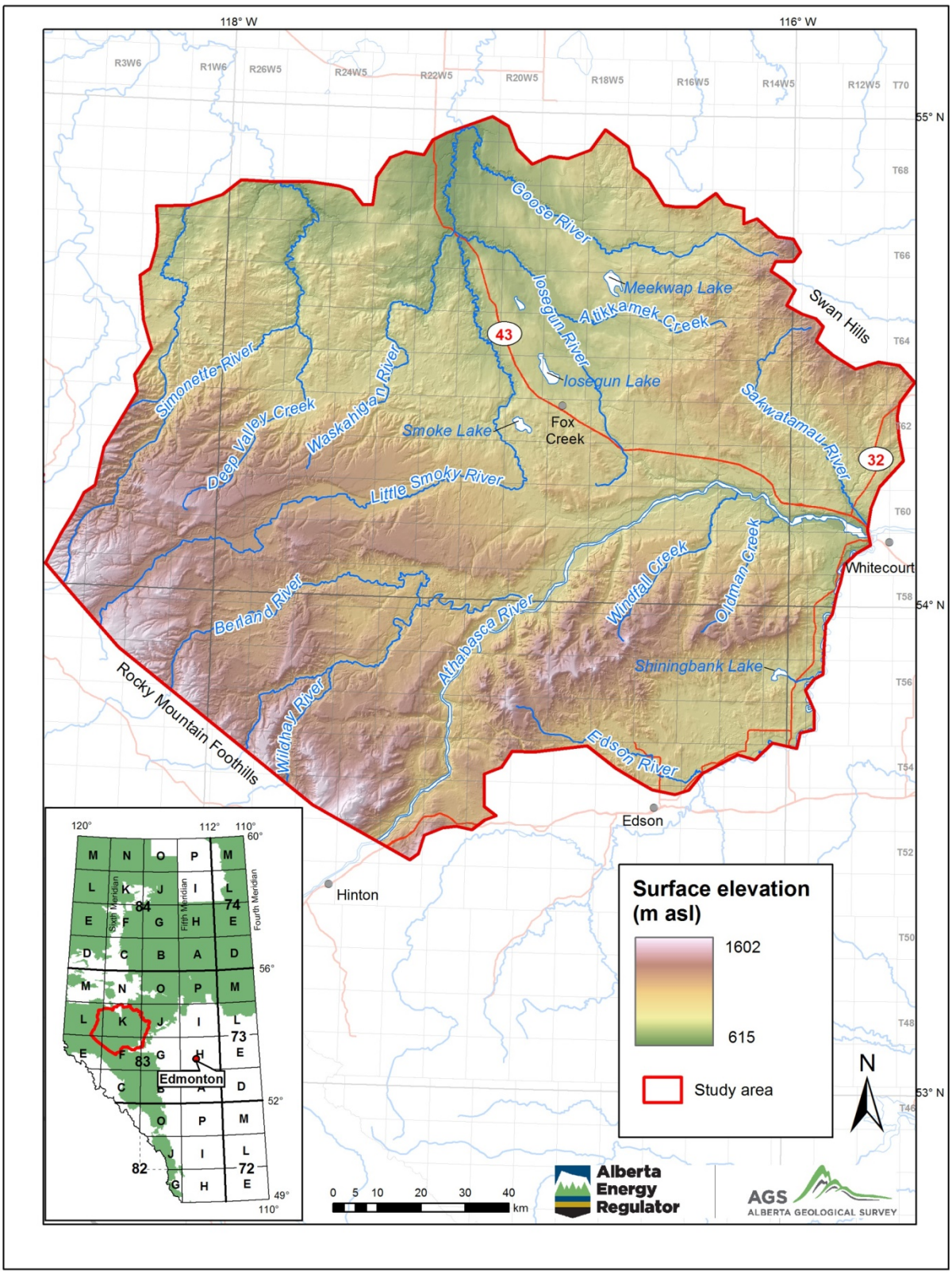

Figure 1. Location of the study area, centred on the Town of Fox Creek, showing a hill-shaded digital elevation model of the land surface (major roads shown as thin red lines). Inset: the green zone is the forested portion of public land in Alberta and the study area is outlined in red.

2 Study Area

2.1 Physical Characteristics and Climate

The 22 170 km^2 study area is centred on the Town of Fox Creek (Figure 1), which is located approximately 260 km northwest of Edmonton. To include active parts of the unconventional shale-gas plays of the Montney and Duvernay formations and maintain a hydrological perspective, the boundary of the study area aligns with hydrological features and spans portions of the Peace River and Athabasca River basins. The southwestern margin of the study area is bounded by the Cordilleran deformation belt, and all other margins are aligned with subbasin drainage boundaries.

The majority of the study area is forested (approximately 94%), unpopulated, and contains infrastructure related to oil and gas production, including roads, well pads, fluid storage facilities (for water and hydraulic fracturing fluids), earthen dams, and pipeline corridors. The physiography of the study area primarily includes benchlands and plains located between the deformation front of the Rocky Mountain Foothills and the Swan Hills (Pettapiece, 1986). The ground surface varies in elevation by almost 1000 m, ranging from a high of about 1600 metres above sea level (m asl) along the southwestern margin of the study area to a low of about 600 m asl in the north. Benchland relief is high, with deep river valley incisions occurring within the step-form character of the landscape. The northern and southeastern parts of the study area and parts of the Athabasca River valley are lower relief plains.

The study area is located in one of the highest precipitation regions within Alberta; it also experiences large spatial variability in precipitation because of the complex relationship between moisture from the Pacific Ocean crossing the Rocky Mountains and the effect of local topography (Mwale et al., 2009). Due to the effects of topography, the precipitation pattern generally mirrors differences in regional physiography, with the highest values in the study area coinciding with the southwestern part of the study area and the lowest values coinciding with the northern part. Weather stations are sparse in the study area; however, long-term climate-normal values can be determined from ClimateNA gridded data (Wang et al., 2016). For the study area, the 1981 to 2010 climate normals for the southwestern margin of the study area were 680 mm/year for precipitation and 500 mm/year for reference evaporation, indicating an average water surplus of 180 mm/year. In the northern portion of the study area, climate normals were 505 mm/year for precipitation and 560 mm/year for reference evaporation, indicating an average water deficit of 55 mm/year. In the Town of Fox Creek, climate normals were 595 mm/year for precipitation and 525 mm/year for reference evaporation, indicating an average water surplus of 70 mm/year. The average water surplus or deficit conditions provide an approximation of the sources and sinks for water in this region, where water surplus drives local river flow and groundwater recharge, and deficit has the potential to remove water from the landscape. The climatic gradient across the study area, combined with long-term hydrometric data for rivers in the region, were the basis for the groundwater yield estimates by Klassen and Smerdon (2018). They found that groundwater recharge varied from a high of 51 mm/year in the southwestern part of the study area to 0 mm/year in the north.

2.2 Geological Setting

The Upper Cretaceous−Paleogene bedrock formations in the study area consist of the Wapiti, Battle, Scollard, and Paskapoo formations (listed from oldest to youngest), which all subcrop towards the northern portion of the study area, with the exception of the Battle Formation (Figure 2).

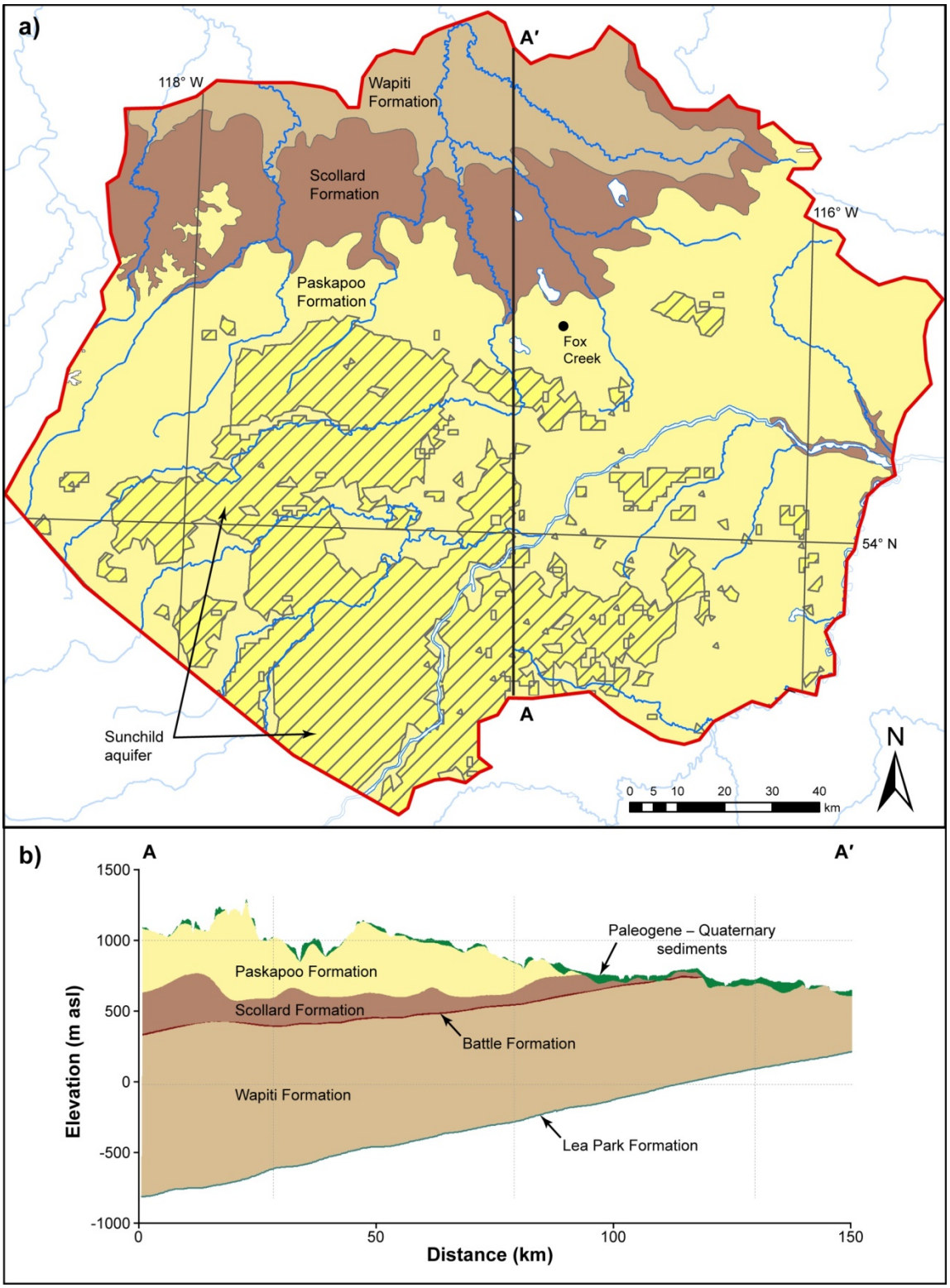

Figure 2. a) Bedrock map of the study area (west-central Alberta) illustrating the extent of the Sunchild aquifer delineated by Lyster and Andriashek (2012). Black line represents location of cross-section A–A′. b) Cross-section A–A′ illustrating the wedge-shaped geometry of bedrock units and relative thickness of the Paleogene–Quaternary sediments, as shown in Babakhani et al. (2019).

The Wapiti Formation is an assemblage of Cretaceous fluvial and floodplain deposits, with localized lacustrine sediments. Dawson et al. (1994) define a lower Wapiti Formation that consists of medium-grained, light grey to brown sandstone, light grey-green siltstone, dark shale, and an absence of coal. The presence of extensive coal seams differentiates the upper Wapiti Formation from the lower Wapiti Formation as described by Dawson et al. (1994), with the upper Wapiti Formation consisting of interbedded medium to light grey, fine-grained sandstone and dark grey mudstone with carbonaceous horizons. Fanti and Catuneanu (2009) suggest that the Wapiti Formation may have five distinct stratigraphic units corresponding to significant changes in major drainage systems during the Cretaceous.

The Battle Formation is a Late Cretaceous deposit of mudstone (Irish, 1970) and is relatively thin (about 10 m thick) or eroded entirely in many places (Hathway, 2011).

The Scollard Formation is a Cretaceous to Paleogene deposit of sandstone and siltstone, interbedded with mudstone (Dawson et al., 1994). The upper portion of the Scollard Formation contains extensive coal seams, which mark the boundary with the overlying Paskapoo Formation.

The Paskapoo Formation is a Paleogene deposit dominated by siltstone and mudstone and interbedded with high permeability coarse-grained channel sandstone (Hamblin, 2004; Grasby et al., 2008). The Paskapoo Formation has been divided into three members by Demchuk and Hills (1991): the Haynes, Lacombe, and Dalehurst members. The lowermost Haynes Member is characterized by thick, massive, coarse-grained sandstone, although this may be restricted to the southern part of the formation's extent (Quartero et al., 2015). The Lacombe Member consists of interbedded siltstone, mudstone, shale, and coal with minor fine- to medium-grained sandstone and is thought to directly overlie the Scollard Formation in the north where the Haynes Member is absent. The overlying Dalehurst Member is present only in the foothills of Alberta and displays interbedded sandstone, siltstone, mudstone, and shale with at least five thick (1.3 to 6.1 m) coal seams.

Paleogene–Quaternary sediments in the study area have recently been studied and represented in a 3D geological model by Atkinson and Hartman (2017). The Paleogene–Quaternary model describes five stratigraphic units (SU) for the study area, including gravel deposits constrained to benchlands (SU1); gravel deposits constrained to plains (SU2); sand or gravel restricted to buried valleys and discrete meltwater channels (SU3); broadly distributed glaciogenic diamict of varying grain size (SU4a); fine-grained sediments associated with deposition in major glacial lakes (SU4b); and sand or gravel confined to modern valleys and glaciofluvial drainage-paths, and eolian deposits (SU5).

Paleogene–Quaternary sediment thickness is highly variable in the study area (Atkinson and Hartman, 2017). Benchlands in the western part of the study have 0 to 5 m of sediment over bedrock. Plains in the northern and southeastern parts of the study area have 25 to 40 m of sediment over bedrock. Where the bedrock has been deeply incised by rivers, discontinuous deposits of sediment can be up to 25 m thick. The bedrock topography in the study area (Atkinson and Hartman, 2017) reveals several paleovalley thalwegs, many of which coincide with modern rivers. Notably, there is a paleovalley underlying the present day Little Smoky River, which appears to have connected with the paleovalley of the present day Athabasca River. However, the present day Little Smoky River changes from a west-east orientation to a south-north orientation in the middle of the study area, only partly following its paleovalley thalweg.

2.3 Hydrostratigraphic Framework

Hydrostratigraphic units (HSUs) can be defined from geological units of similar texture, geological history, and sufficient lateral continuity to be mapped at a regional scale (1:100 000). For this study, HSUs were defined from the findings of Atkinson and Hartman (2017) for the unconsolidated Paleogene–Quaternary sediments and Babakhani et al. (2019) for the consolidated bedrock units.

The 3D stratigraphic model (Table 1; Figure 3) by Atkinson and Hartman (2017) was based on lithology, stratigraphic and topographic position, genesis, and depositional setting. Only units that were recognized and mappable at the regional scale were included in the model, making the stratigraphic units (i.e., SU1 to

SU5) ideal hydrostratigraphic units. Each of the units delineated has a description that can be qualitatively correlated to hydrogeological properties (Table 1), and the 3D model provides thickness and extent for each of these Paleogene–Quaternary units in the study area.

Within the bedrock units, division of the Paskapoo Formation has previously been based on the occurrence of sandstones, resulting in three informal hydrostratigraphic units suggested by Lyster and Andriashek (2012): the Haynes and Sunchild aquifers and the Lacombe aquitard. The Haynes aquifer and Lacombe aquitard units correlate to the Haynes and Lacombe Members, respectively, as proposed by Demchuk and Hills (1991). The Sunchild aquifer is suggested to be correlative to the Dalehurst Member and is characterized by permeable sandstone bodies that display variable interconnectivity due to stacked sandstone structure and incision by present-day rivers (Lyster and Andriashek, 2012). These informal hydrostratigraphic units provide unique descriptions that are applicable and generally understood by geoscientists that work in the study area.

The 3D model of the bedrock hydrostratigraphy (Figure 4) by Babakhani et al. (2019) was developed from combining data sourced from gamma-ray logs from oil and gas wells and lithological descriptions from water wells. The model provides a rendering of sandstone abundance for the study area and includes the Lea Park, Wapiti, Battle, Scollard, and Paskapoo formations. A wide variation in sandstone abundance was found, where zones with abundant sandstone are likely to be local aquifers within the more dominant siltstone-mudstone sediments of the same geological formation.

As described in Babakhani et al. (2019), and depicted in Figure 4b, there are regional trends in sandstone abundance that have important implications for groundwater resources in this region, including

- a nearly continuous and approximately 230 m thick sandstone-dominated unit in the basal portion of what has otherwise been an undifferentiated Wapiti Formation;
- a slightly discontinuous and approximately 200 m thick mudstone/shale unit within the middle portion of the undifferentiated Wapiti Formation, which terminates in the northern part of the study area;
- the absence of a basal sandstone-dominated unit (i.e., Haynes aquifer) within the Paskapoo Formation;
- sandstone abundance in the uppermost portion of the Paskapoo Formation, confirming the presence of the Sunchild aquifer described by Lyster and Andriashek (2012); and
- the dominance of siltstone and mudstone in the bedrock, with the net sandstone to gross interval thickness (referred to as net-to-gross ratio [NGR]) of less than 0.5.

Table 1. Qualitative hydrogeological properties of Paleogene−Quaternary stratigraphic units (SU), Fox Creek area, west-central Alberta.

Unit	Geological Description	Hydrogeological Property	
		Material	Relative Hydraulic Conductivity
SU5	Fluvial, glaciofluvial, sand and gravel, or eolian sand	Sand and/or gravel	High
SU4b	Fine-grain diamict, silt and clay, or glacially disturbed bedrock	Silt and clay	Low
SU4a	Diamict (varied grain size); silt and clay; glacially reworked or displaced bedrock	Sand and silt with minor clay	Medium
SU3	Sand and/or gravel resting on the floors of bedrock valleys	Sand and/or gravel	High
SU1 and SU2	Gravel overlying bedrock	Gravel	High

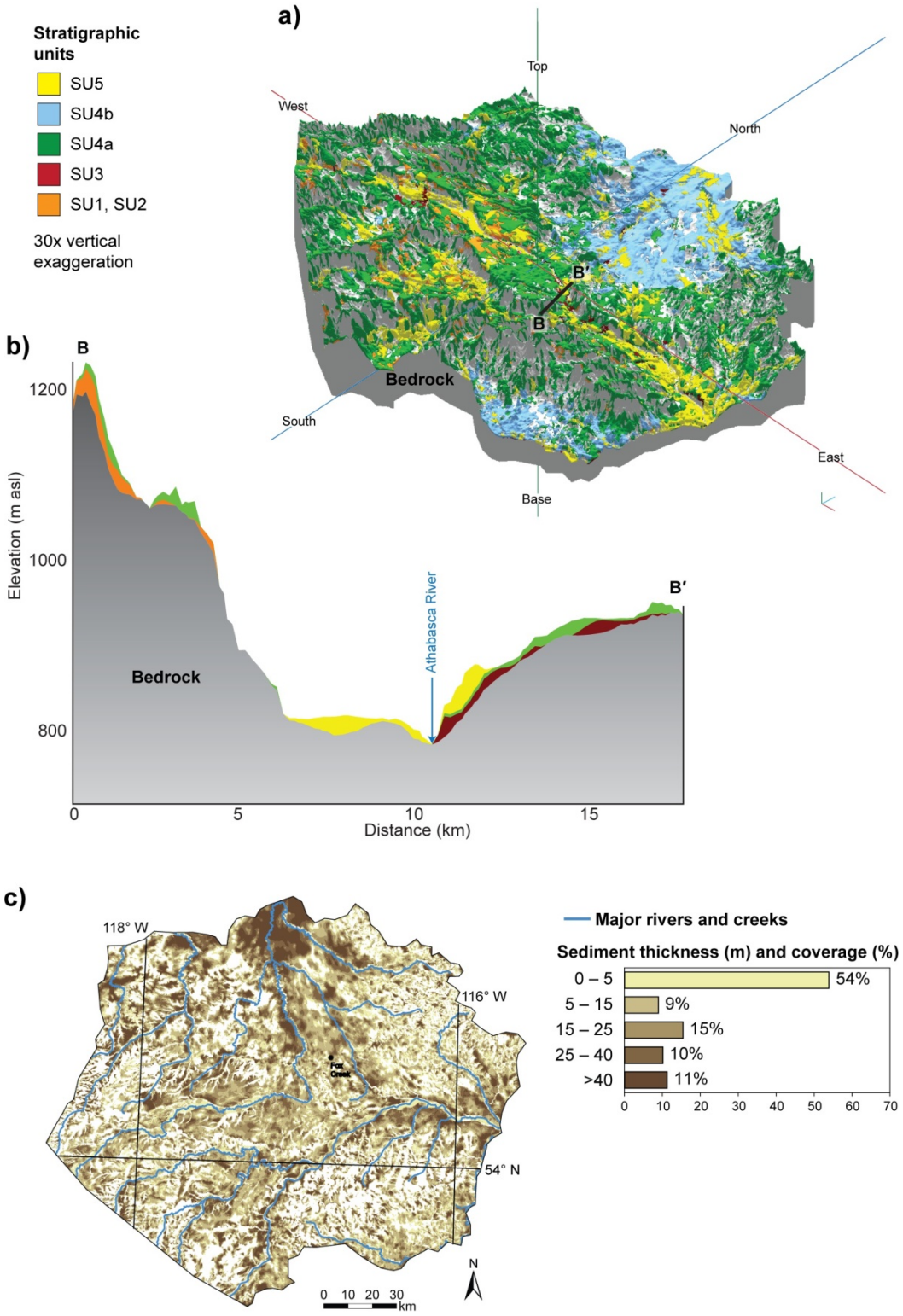

Figure 3. Summary of Paleogene−Quaternary model by Atkinson and Hartman (2017), Fox Creek area, west-central Alberta: a) three-dimensional (3D) view of stratigraphic units; b) cross-sectional distribution of sediments across the Athabasca River valley; c) distribution of sediment thickness in the study area. Abbreviation: SU, stratigraphic unit.

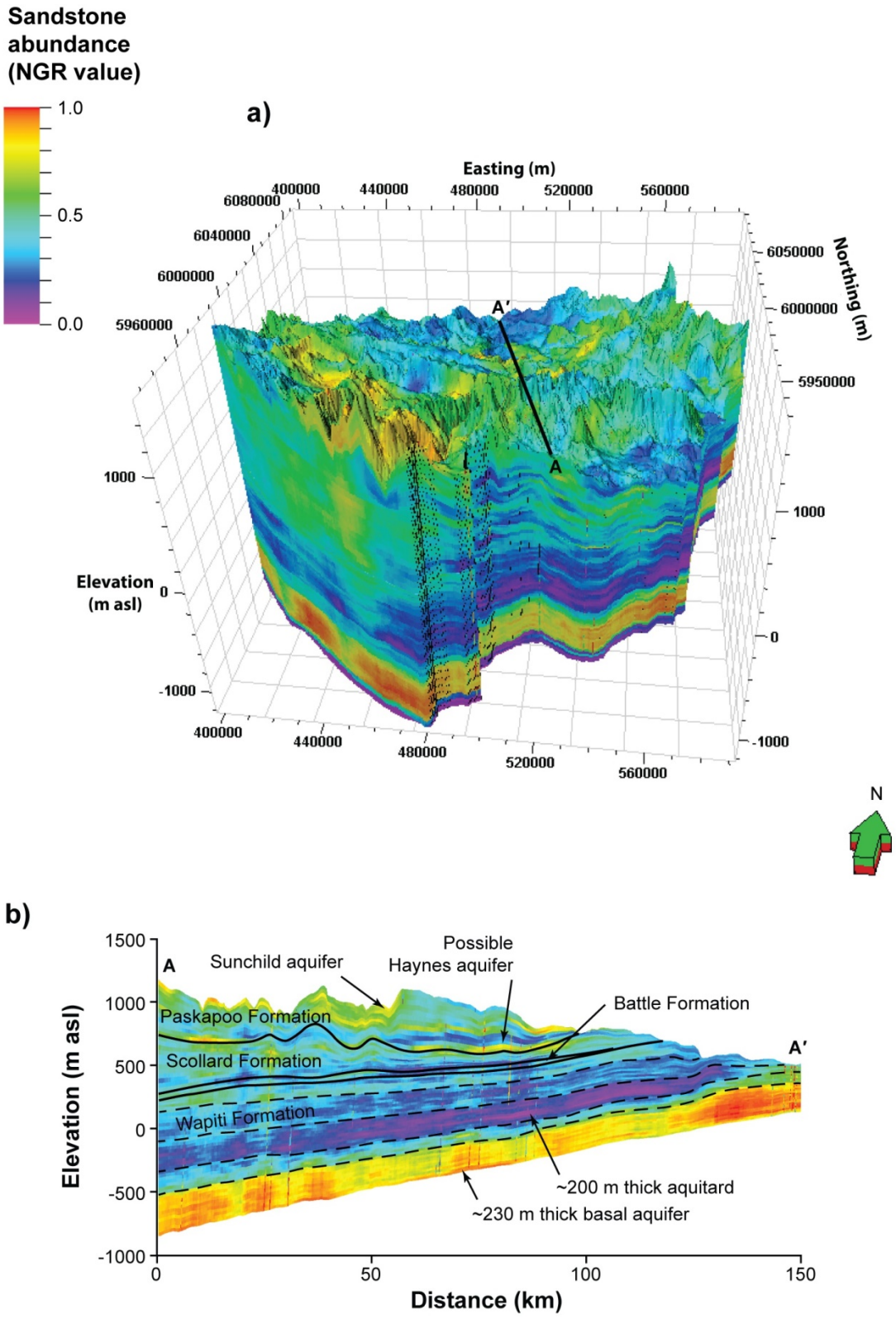

Figure 4. a) Three-dimensional (3D) view of modelled bedrock sandstone abundance (expressed as net-to-gross ratio [NGR] value), west-central Alberta, by Babakhani et al. (2019). b) Cross-sectional distribution of sandstone abundance through the study area with example hydrogeological units by Babakhani et al. (2019).

2.4 Hydraulic Properties

The 3D hydrostratigraphic framework provided by the models of Atkinson and Hartman (2017) and Babakhani et al. (2019) contributes to an understanding of the relative ability of specific geological formations and internal units (e.g., extensive sand/sandstone bodies) to store and transmit water. To quantify rates of groundwater movement, knowledge of the hydraulic properties for the HSUs are needed as well.

Measured hydraulic properties for the unconsolidated Paleogene–Quaternary sediments are generally unknown; however, the approximate hydrogeological properties (Table 1) can be used to estimate hydraulic conductivity and porosity values.

For the consolidated bedrock units, measured values are available and summarized here. Hughes et al. (2017a) provide the most recent and comprehensive summary of hydraulic properties for the Paskapoo Formation, including permeability testing completed on rock cores located within the study area (Hughes et al., 2017b). Mean hydraulic conductivity values based on air-permeametry were 1.3×10^{-6} m/s for sandstone (Figure 5a) and 4.4×10^{-9} m/s for mudstone (Figure 5b). Following the HSUs suggested by Lyster and Andriashek (2012), these hydraulic conductivity values would correspond to the Sunchild aquifer and Lacombe aquitard, respectively. Hydraulic conductivity estimated from pumping test data (Hughes et al., 2017b) was found to be 2.4×10^{-4} m/s for the Paskapoo Formation in the study area. It should be noted that values determined by air-permeametry are often lower than pumping tests, due to a difference in scale of measurement. Pumping tests often have higher hydraulic conductivity values than those determined in laboratory settings due to inclusion of larger scale heterogeneity (e.g., fractures) and bias towards testing more permeable zones suitable for water supply.

For the Wapiti Formation, hydraulic property information was obtained from AccuMap™ (IHS Markit, 2018). The maximum permeability values (representing horizontal permeability) were converted to hydraulic conductivity and grouped based on two depth intervals to differentiate parts of the Wapiti Formation that may interact with surface water and be available for typical nonsaline applications (e.g., common water well depths). Mean hydraulic conductivity values for the 0 to 500 m (Figure 5c) and 500 to 1000 m (Figure 5d) depth intervals were 7.1×10^{-6} and 3.8×10^{-6} m/s, respectively. Although the mean values are similar, the median values (2.6×10^{-6} and 2.6×10^{-8} m/s) indicate that the uppermost 500 m of the Wapiti Formation may have higher hydraulic conductivity than the 500 to 1000 m depth. Additional analysis is needed to better understand the relation of hydraulic property information and heterogeneity of modelled sandstone abundance in the Wapiti Formation.

For the Paskapoo Formation, Hughes et al. (2017a) found that porosity values range from 0.02 to 15% with an average of 5% for the Sunchild aquifer, and Grasby et al. (2007) found that porosity values range from 4 to 33% with an average of 19% for the Haynes aquifer. A positive relationship between porosity and hydraulic conductivity exists (Figure 5e). For the Wapiti Formation, mean porosity values from AccuMap™ (IHS Markit, 2018) were 22% for the 0 to 500 m depth interval and 19% for the 500 to 1000 m depth interval. Similar to hydraulic conductivity, the median porosity for the uppermost 500 m was higher (26%) than the 500 to 1000 m depth (18%), leading to a positive relationship between porosity and hydraulic conductivity (Figure 5f).

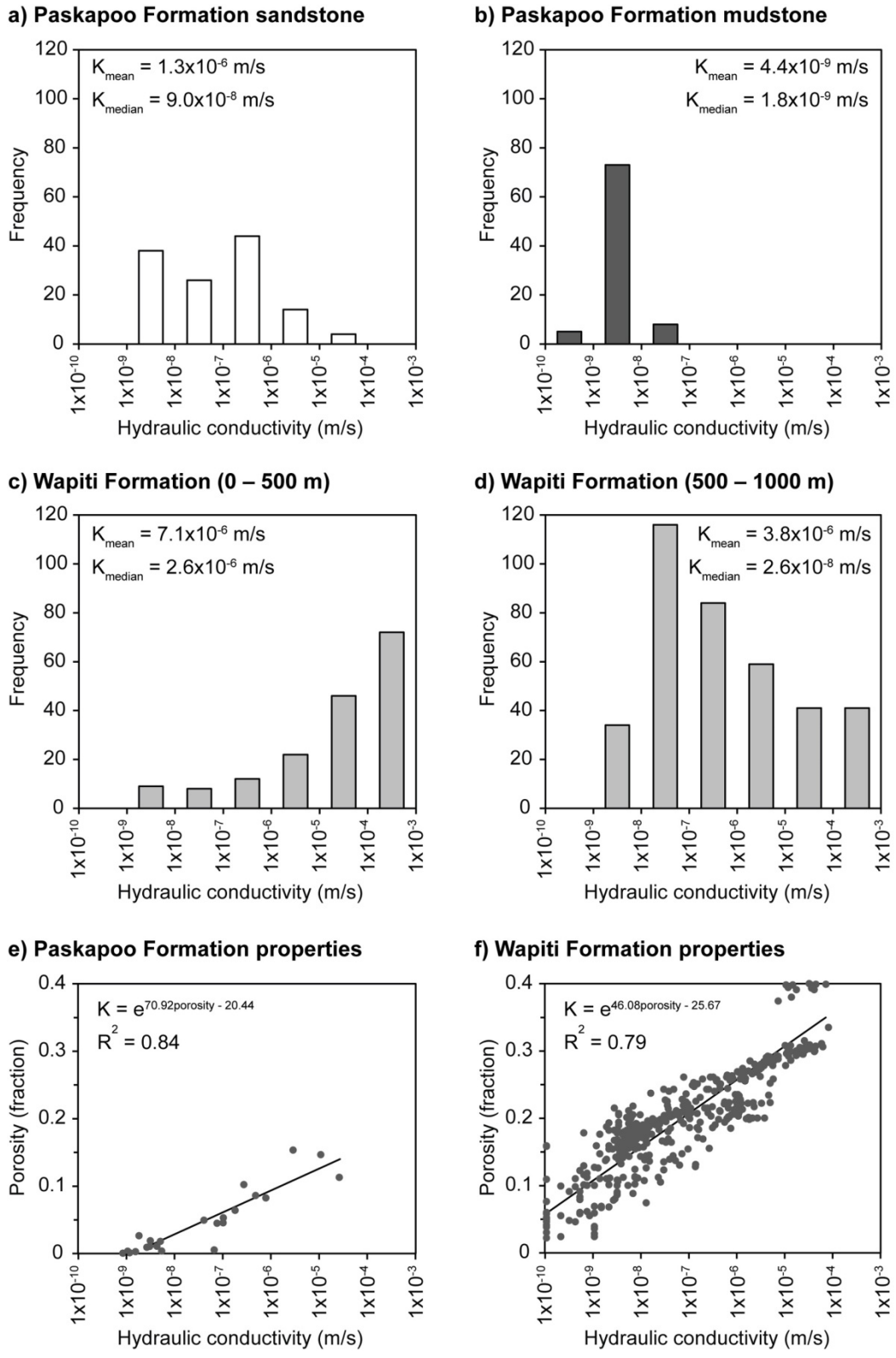

Figure 5. Summary of hydraulic property data for the Paskapoo and Wapiti formations within the study area, west-central Alberta. Values for mean and median hydraulic conductivity denoted by K_{mean} and K_{median}. Abbreviations: e, natural exponential function; K, hydraulic conductivity; R^2, coefficient of determination.

3 Hydrogeological Mapping

To assess regional hydrogeological conditions, groundwater data from the Alberta Water Well Information Database (AWWID; Alberta Environment and Parks, 2018) and legacy information from the Alberta Research Council (ARC) held in internal AGS data holdings were assembled to

- interpret the hydraulic head data to produce a potentiometric surface map for the uppermost bedrock units,
- estimate the vertical hydraulic head gradients and groundwater flow potential, and
- visually represent total dissolved solids (TDS) concentration for water wells in the region.

3.1 Potentiometric Surface

Water wells completed in the unconsolidated Paleogene–Quaternary sediments were sparse, scattered throughout the study area, and generally limited to locations where the sediments were thick and relatively permeable (e.g., gravel dominated SU1, SU2, and SU5 shown on Figure 3). The sporadic nature of water wells completed in the unconsolidated Paleogene–Quaternary sediments precluded interpolation to develop any potentiometric surface maps for these units.

Water level information was extracted from the AWWID and went through screening criteria to select wells with appropriate information (i.e., culling). Water wells were chosen if 1) the water level data were more recent than January 1, 2000, 2) they were not under flowing artesian conditions, 3) they were screened in bedrock, and 4) they did not contain duplicate screen intervals or water level measurements. In total, 1742 wells were used to interpolate a potentiometric surface in ArcGIS using the ordinary kriging function of the Geostatistical Analyst extension using a 200 m digital elevation model (DEM; Figure 6). A depth to potentiometric surface map (Figure 7) was created by subtracting the bedrock potentiometric surface map (Figure 6) from a 200 m DEM of the land surface (Atkinson and Hartman, 2017).

The bedrock potentiometric surface reflects ground surface topography in the Fox Creek area, as expected for a region having a moderate level of precipitation. Groundwater flow is driven from higher elevation areas along the southwestern part of the study area (deformation belt) and the Swan Hills in the northeast, towards the north. The major exception being the Athabasca River valley along the southeastern margin of the study area, which is a dominant drainage feature for surface water and shallow groundwater in the study area. Across many of the elevated plateaus, the potentiometric surface is relatively level.

The depth to potentiometric surface map illustrates the likelihood of encountering groundwater emerging at the ground surface, and is shown along with the occurrence of known springs in Figure 7. Shallow groundwater appears to be constrained to river valley corridors and localized wetland areas on upland plateaus in the southwestern portion of the study area.

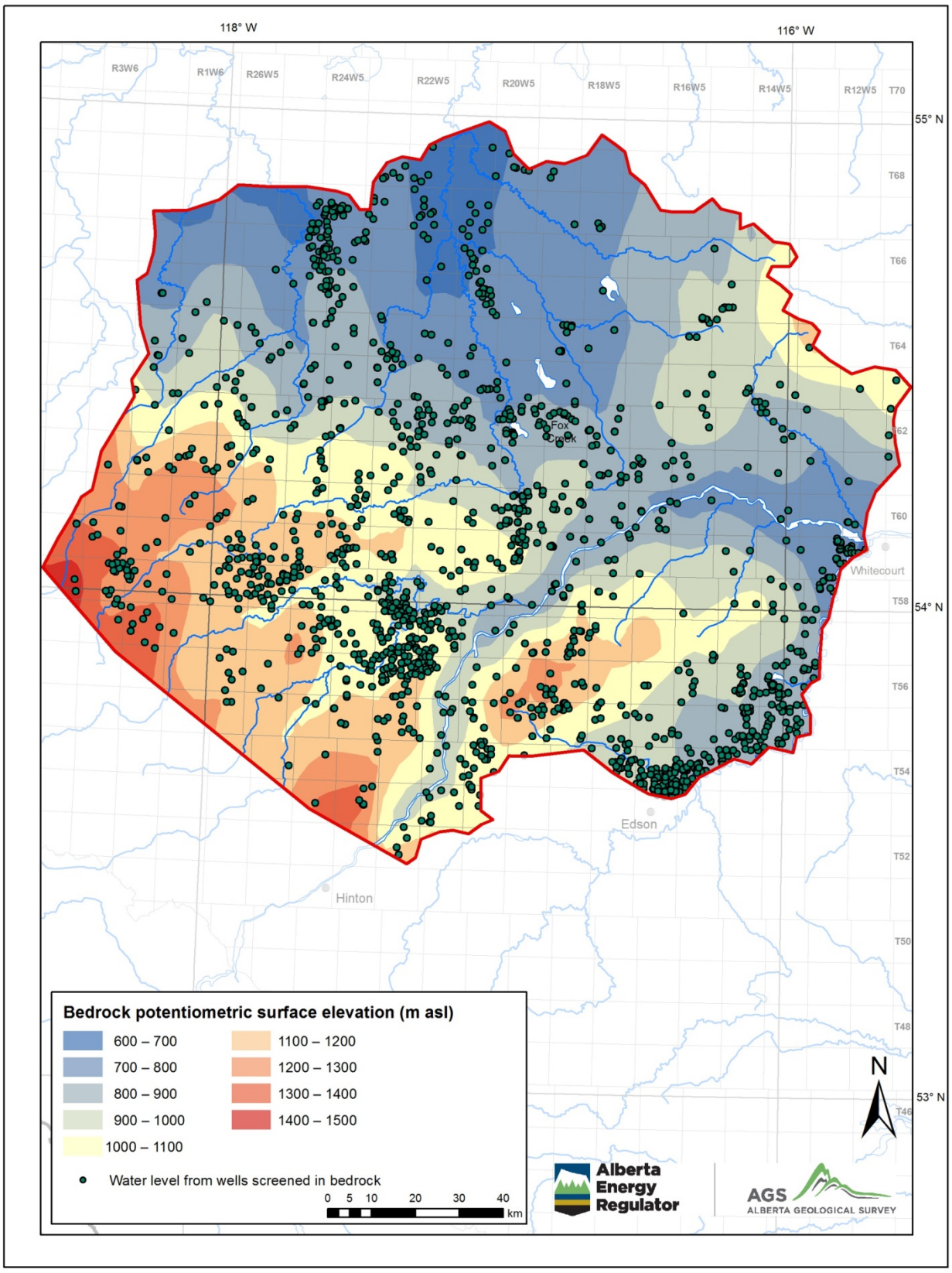

Figure 6. Potentiometric surface for the uppermost bedrock units in the study area, west-central Alberta.

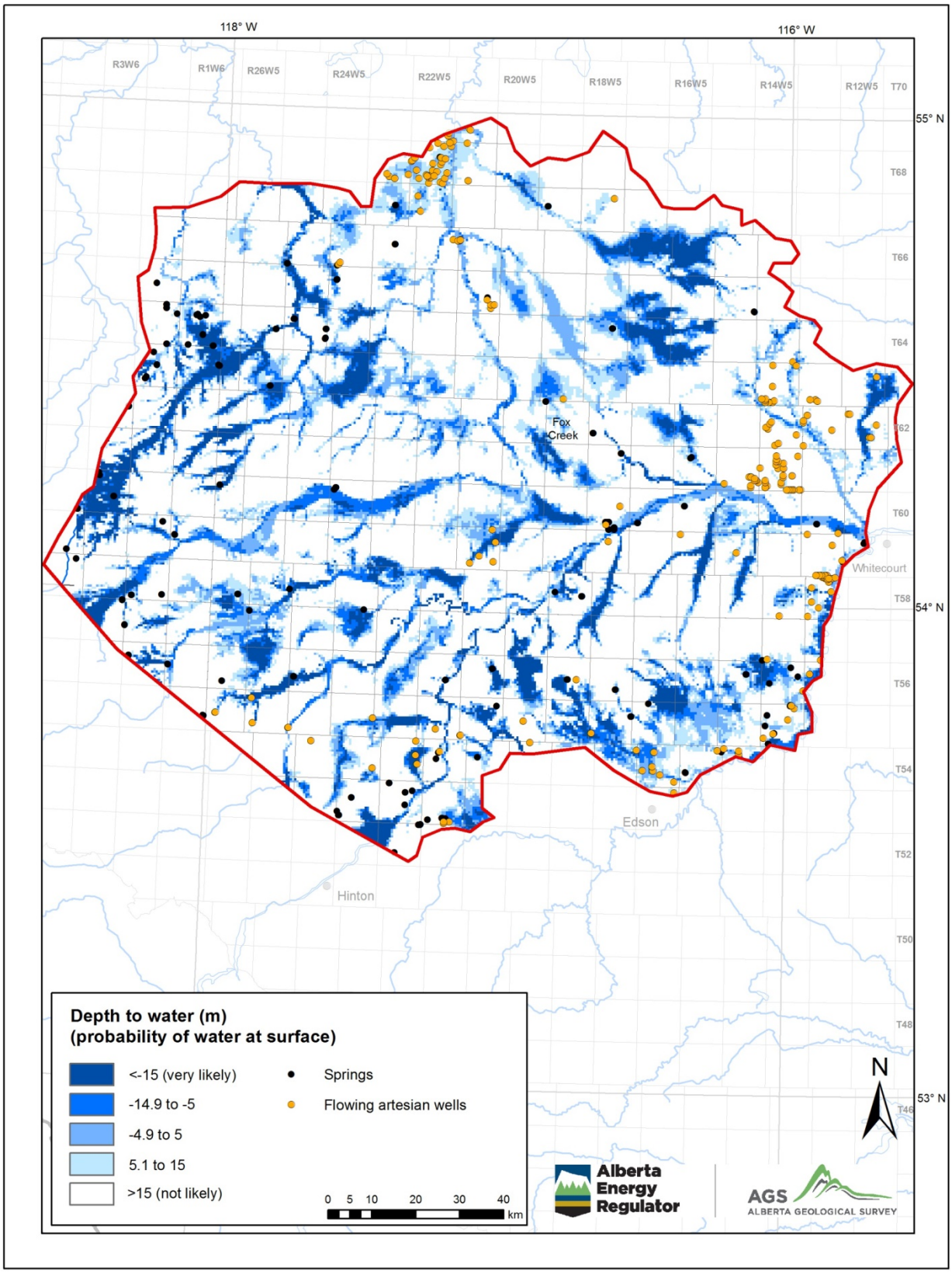

Figure 7. Depth to potentiometric surface for the uppermost bedrock units in the study area, west-central Alberta.

3.2 Vertical Hydraulic Gradients

To assess the spatial distribution of recharge and discharge, vertical hydraulic head gradients were examined. The vertical gradient is defined by the difference in hydraulic head divided by the difference in elevation between where the hydraulic heads are measured. The resultant values are unitless and indicate the potential for downward or upward groundwater flow (i.e., groundwater recharge or discharge conditions).

Water level information was extracted from the AWWID without applying the criteria used to develop the potentiometric surface map, with an intention to capture more information, including sporadic data in Paleogene–Quaternary sediments, and a longer period of record. Water well data were removed if they were not located within a legal subdivision or if a GPS had not been used to document location coordinates. Water well data were also removed if wells could not be paired to create a set of nested wells (i.e., two to three wells of varied depth in close proximity). If multiple water wells had screened intervals at the same depth, the most recent sample date was chosen for analysis. In total, 5085 wells were used to estimate vertical hydraulic head gradients across the study area.

Water wells were organized into nested wells based on location within sections and quarter townships. The gradient was calculated for each set of nested wells and where there was more than one set of nested wells within a section or quarter township, the average gradient was calculated and used to represent that area (Figure 8). Negative vertical gradients represent upward flow potential and positive vertical gradients represent downward flow potential.

Most of the sections or quarter townships indicate the potential for downward flow (groundwater recharge). Upward flow (groundwater discharge) is likely to occur on a more localized scale around surface water bodies and identified springs (Figure 8).

Although this approach to assessing the spatial distribution of recharge and discharge is applicable for regional studies having sparse information, several limitations must be understood:

- it does not take into consideration the presence or absence of confining layers that can inhibit movement of groundwater,
- the approach is not continuous throughout the study area and therefore only provides estimates in specific areas due to spatially limited water well data,
- the presence of known springs and flowing artesian wells may represent other hydraulic mechanisms that are not captured in the vertical gradient analysis,
- this map only indicates the potential for groundwater flow and not actual groundwater flow.

3.3 Groundwater Chemistry

Chemical analyses that included major-ion chemistry and TDS were compiled from three sources: the AWWID; previous groundwater sampling by the Alberta Research Council (i.e., legacy data holdings); and four groundwater samples collected by the AGS as part of this study (described in Section 5). TDS was determined by summing the concentration of major ion constituents for results that met selection criteria. The criteria included charge balance error of ±5%, water well construction information (e.g., known screened interval), and screened intervals less than 15 m. Chemical data were predominantly found for the Paskapoo Formation, and thus limited to this geological unit. The chemical data were considered too sparse to interpolate over the extent of the study area; however, the data have been plotted on a piper diagram (Figure 9) and spatially for TDS (Figure 10) to provide a basic understanding of groundwater chemistry.

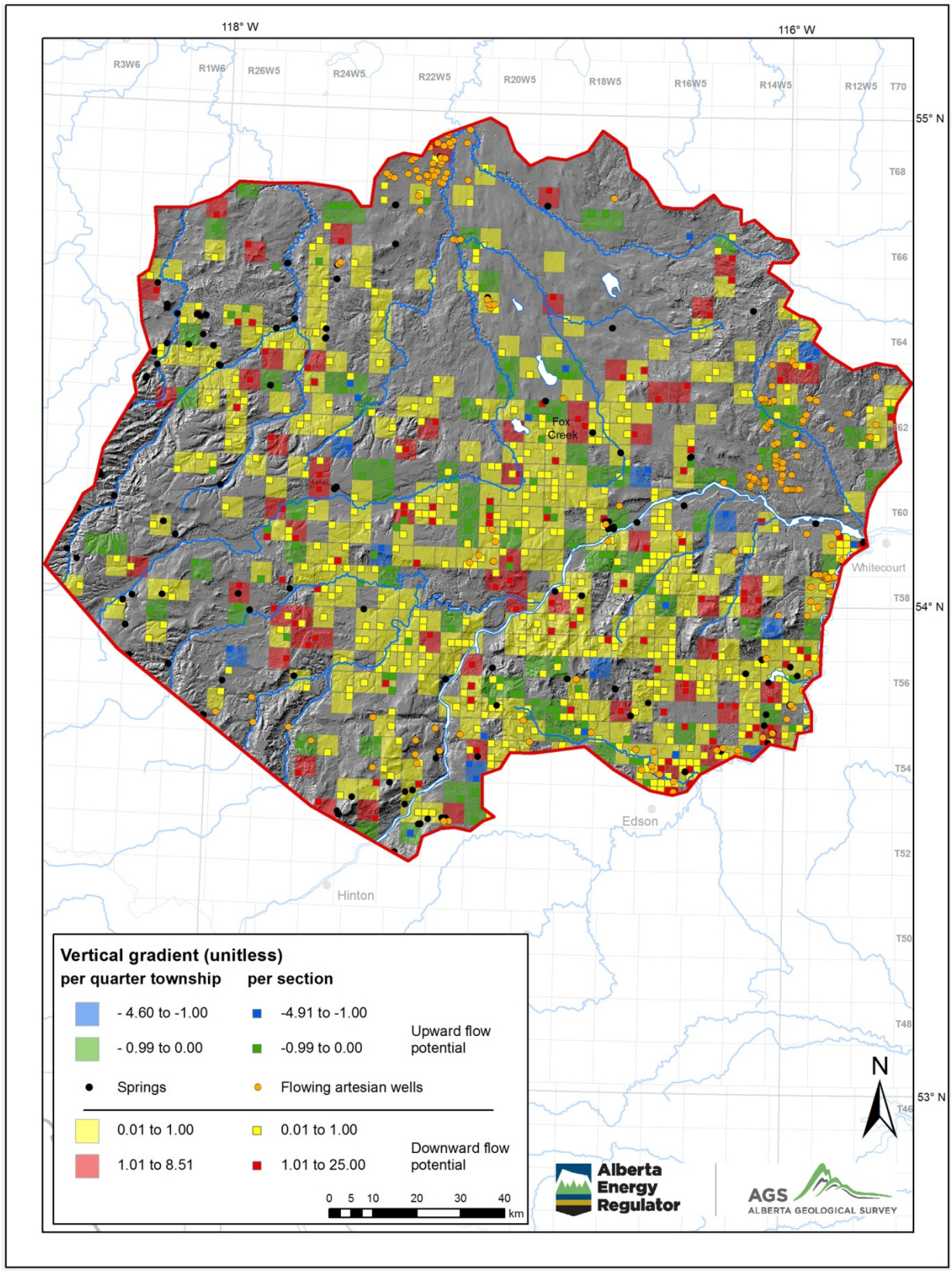

Figure 8. Vertical hydraulic head gradients per quarter township (large squares) and per section (small squares), Fox Creek area, west-central Alberta.

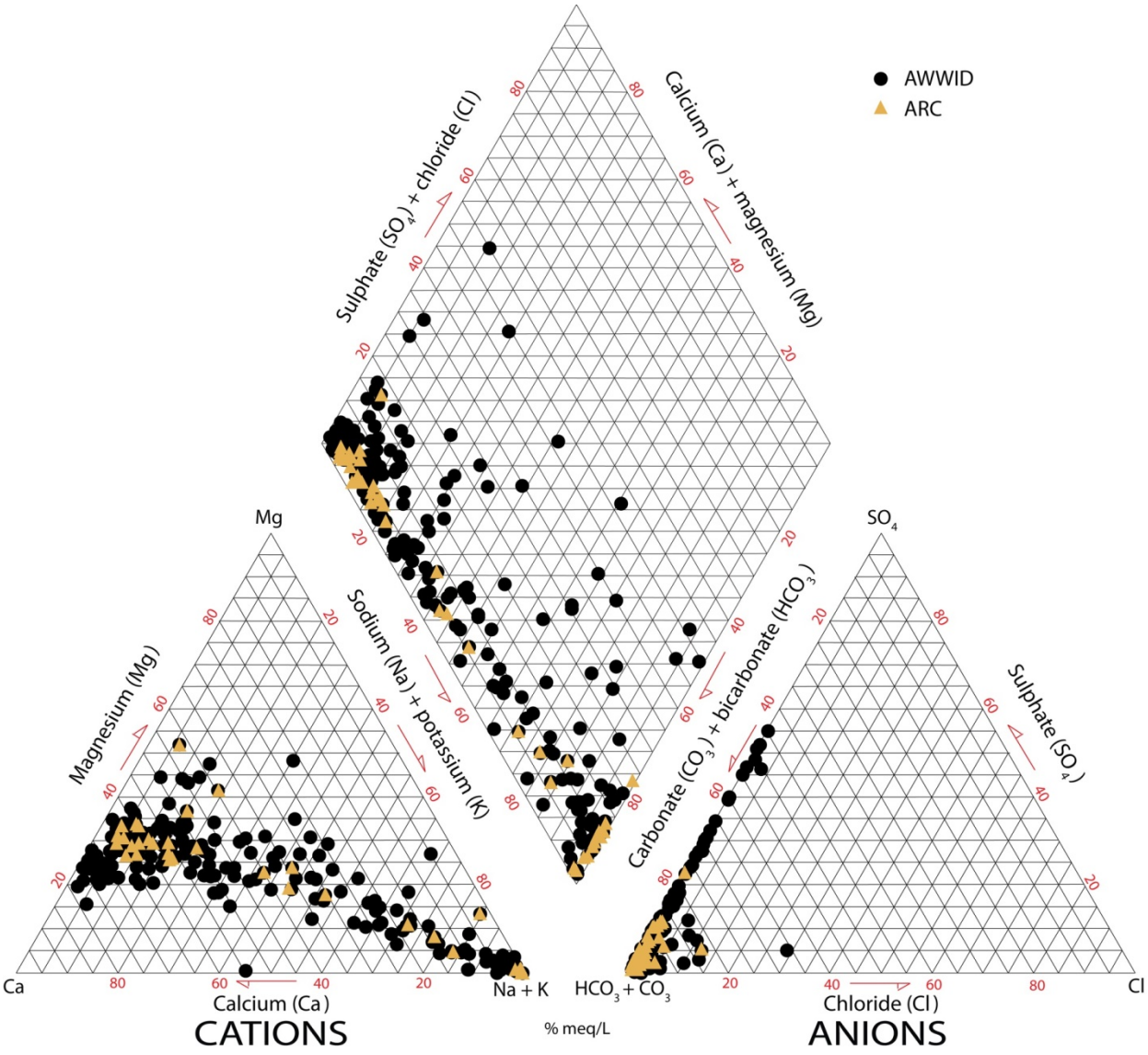

Figure 9. Piper diagram of groundwater chemistry of the Paskapoo Formation in the Fox Creek area, west-central Alberta. Data from Alberta Research Council (ARC) legacy data holdings and Alberta Water Well Information Database (AWWID; Alberta Environment and Parks, 2018). Abbreviation: meq, milliequivalent.

Across the majority of the study area the TDS concentration is 500 mg/L or less, with only a few locations having higher concentrations of TDS. At the northern margin of the Paskapoo Formation and in the southeastern part of the study area (near Edson and Hinton, Alberta), the TDS concentration is up to 1000 mg/L, with a few locations having even higher TDS concentrations. The piper diagram illustrates dominance of HCO_3+CO_3 waters that appear to follow the groundwater evolution path of $CaMgHCO_3$ to $CaMgSO_4$; however, the poor spatial distribution of chemical analyses precludes any further analysis and interpretation.

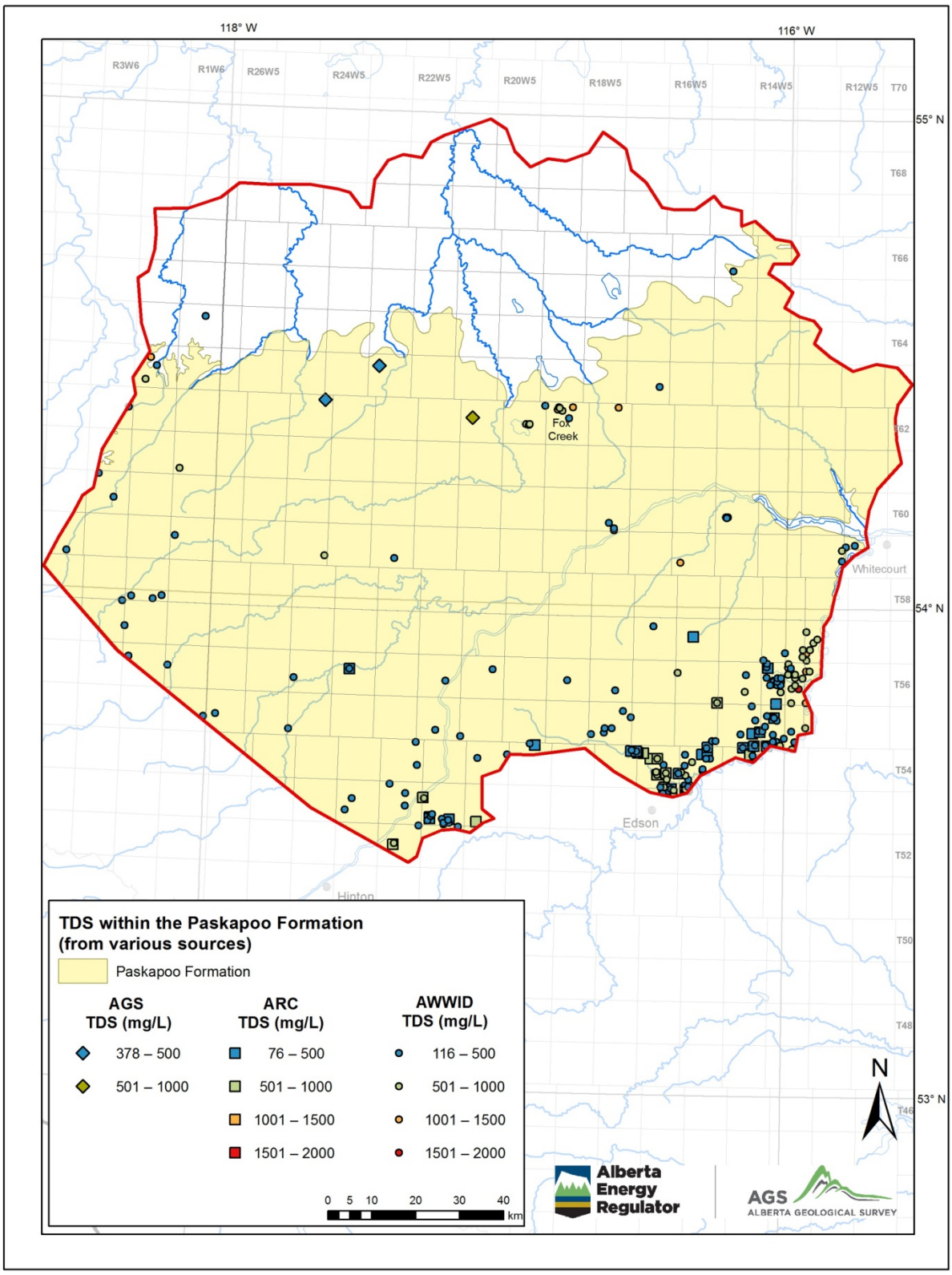

Figure 10. Concentration of total dissolved solids (TDS) in the Paskapoo Formation (Fox Creek area, west-central Alberta) from the current study by the Alberta Geological Survey (AGS), and from previous sampling by the Alberta Research Council (ARC) and Alberta Water Well Information Database (AWWID; Alberta Environment and Parks, 2018).

4 Regional Hydraulic Pathways

A GIS-based indexing approach for mapping regional hydraulic pathways was developed using the geological attributes described in Section 2. These pathways identify locations where permeable Paleogene–Quaternary sediments and permeable bedrock coincide, providing a potential for enhanced vertical groundwater movement. These regional hydraulic pathways were defined from a combination of the lateral extent and thickness of Paleogene–Quaternary stratigraphic units (Figure 3a) and bedrock sandstone abundance (Figure 4a).

4.1 Geological Attributes

The GIS-based indexing approach assigned qualitative ratings to geological attributes from a hydrogeological perspective. Low rating values indicate the potential of the geological materials to more readily transmit groundwater vertically than high rating values. The ratings only consider the capacity of the geological materials and do not consider specific hydrogeological conditions, such as the potentiometric surface and vertical hydraulic head gradient described in Section 3. This section describes how rating values were defined to account for some of the geological complexity in the study area.

The Paleogene–Quaternary stratigraphic units SU1 and SU2 represent gravel that directly overlies bedrock on step-form benchlands and the two units were combined for this study. SU3 is sand and/or gravel deposits located on the floor of bedrock valleys. SU4a is the most complex unit as it differs greatly throughout almost the entire study area; the unit is dominantly a matrix-supported sand to silt diamict with minor silt and clay. SU4b material is finer textured than SU4a and includes both clay-rich diamict and massive to laminated clay and silt deposited or reworked by glacial and/or glaciolacustrine processes. The final unit, SU5 is composed of fluvial and glaciofluvial sand and/or gravel, and eolian sand.

For the GIS-based indexing approach, units SU1 through SU5 (with SU2 being combined with SU1) were assigned a relative rating based on the approximate hydraulic conductivity (see Table 1). Ratings took into consideration the material and thickness of each unit from a hydrogeological perspective. Material ranged from silt and clay to sand and gravel and thickness was divided into less than 5 m, 5 to 10 m and greater than 10 m intervals (Table 2). The rating scheme for Paleogene–Quaternary stratigraphic units varied from 1 to 15 and indicates the potential for hydraulic communication (Figure 11a); whereby a low rating indicates high potential for hydraulic communication through the Paleogene–Quaternary stratigraphic units and a high rating indicates low potential for hydraulic communication. Thin, permeable units were assigned a low rating to represent a potential for vertical groundwater movement and thick, less permeable units were assigned a high rating. The rating assigned was on a scale larger than 1 to 5 in order to account for the influence of the different material types. For example, SU4b is a very thick unit of silt and clay, and is likely much less permeable compared to the gravel of SU1, which directly overlies bedrock and is therefore more likely to function as a hydraulic pathway. The ratings were summed to create a map with a rating of 1 to 31; the map was then reclassified to a rating of 1 to 5 (Table 3; Figure 11b).

Table 2. Rating scheme for five stratigraphic units (SU) identified within the Fox Creek area, west-central Alberta.

Unit	Material	Rating		
		<5 m	5–10 m	>10 m
SU5	Sand and/or gravel	2	3	4
SU4b	Silt and clay	13	14	15
SU4a	Sand and silt with minor clay	8	9	10
SU3	Sand and/or gravel	1	2	3
SU1 and SU2	Gravel	1	2	3

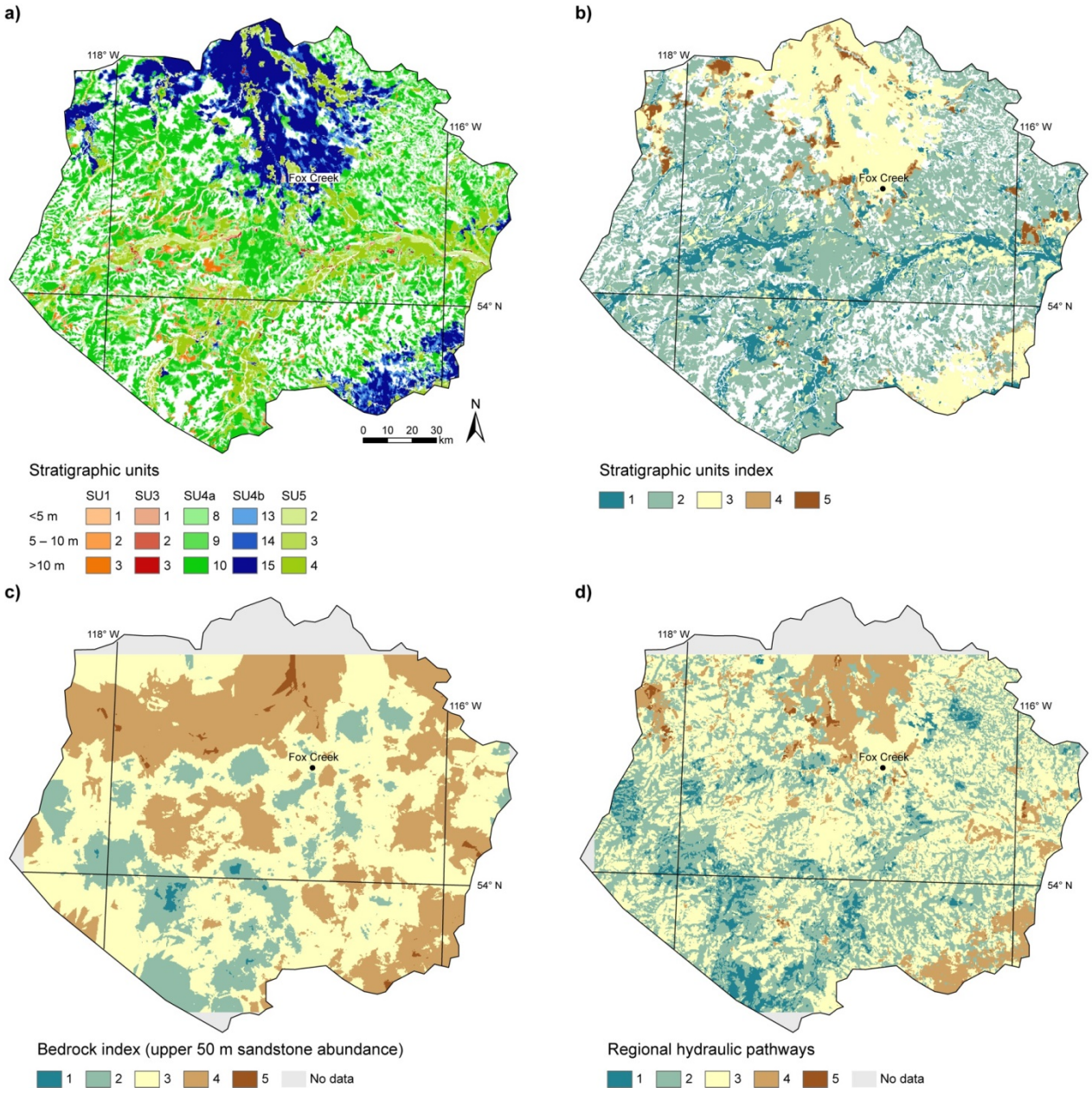

Figure 11. a) Rating assigned to five mappable stratigraphic units (SU), where SU2 has been included with SU1; b) hydraulic pathways derived from stratigraphic unit classification where blue generally represents thin, coarse sediment and brown represents thick, fine sediment; c) hydraulic pathways derived from the uppermost 50 m of the bedrock where blue represents a high sandstone abundance and brown represents a low sandstone abundance; d) distribution of hydraulic pathways where blue represents high likelihood of vertical groundwater movement and brown represents low likelihood of vertical groundwater movement; Fox Creek area of west-central Alberta.

For the bedrock sandstone abundance, the data were in the form of point data with a depth and net-to-gross ratio (NGR) of sandstone. In order to calculate the average sandstone abundance for the top 50 m of bedrock, the point data depths were subtracted from the bedrock surface. Points where the depth was greater than 50 m were removed. When multiple points were present at one location, the weighted average NGR was calculated for that point. Once an average NGR value was known for each point within the study area, the sandstone abundance for the top 50 m of bedrock was interpolated by ordinary kriging. The ratings assigned to NGR values are shown in Table 4 and Figure 11c. It should be noted that the bedrock geological model did not extend to cover the northernmost portion of the study area; however, the bedrock formations in this area are predominantly mudstone and were assumed to have a low NGR value.

4.2 Hydraulic Pathway Indexing

The stratigraphic units and bedrock index maps were summed and reclassified (Table 5) to create a regional hydraulic pathway map (Figure 11d). This map identifies potential permeable pathways for vertical groundwater movement through Paleogene–Quaternary deposits and the uppermost 50 m of bedrock in the study area. The likelihood of a permeable pathway is on a scale from 1 (dark blue) to 5 (dark brown); 1 representing areas with a high likelihood and 5 representing areas with a low likelihood of being a permeable vertical hydraulic pathway.

Table 3. Reclassification of materials comprising stratigraphic units to a rating scale of 1 to 5, Fox Creek area, west-central Alberta.

Stratigraphic Output	Reclassified Rating
1–5.9	1
6–11.9	2
12–17.9	3
18–23.9	4
24–31	5

Table 4. Rating scheme for top 50 m of bedrock in the Fox Creek area, west-central Alberta. Abbreviation: NGR, net-to-gross ratio.

Bedrock NGR Value	Rating
0–0.19	5
0.2–0.39	4
0.4–0.59	3
0.6–0.79	2
0.8–1	1

Table 5. Reclassification of hydraulic pathways to unit rating of 1 to 5, Fox Creek area, west-central Alberta.

Hydraulic Pathway Value	Rating
9-10	5
7-8	4
5-6	3
3-4	2
1-2	1

5 Surface Water–Groundwater Interaction

The headwaters of many tributaries draining into the Peace River and Athabasca River basins rely on baseflow sourced primarily from bedrock formations in the study area. The source of baseflow is an important, yet understudied component of the groundwater cycle. Groundwater is needed to maintain low flows in these rivers, which is critical for environmental conditions that sustain in-stream aquatic habitat and the near-stream ecological state. To better understand the interaction between surface water and groundwater, three river systems were examined as part of this study, including the Little Smoky River, the Deep Valley Creek–Simonette river system, and Wildhay–Berland river system. Two of the river systems comprise tributaries that merge within the study area, with Deep Valley Creek joining the Simonette River and the Wildhay River joining the Berland River (Figure 1).

5.1 Water Sampling and Analytical Methods

Several techniques exist for identifying the location and rate of groundwater interaction with rivers. Many common methods use hydrograph analyses or chemical and isotopic separation techniques, often at the location of long-term river gauging stations. However, in-river methods such as synoptic water sampling (e.g., Harrington et al., 2013) offer the ability to learn more about the internal dynamics within a river basin, including surface water and groundwater interaction at the regional scale. Measurements of water chemistry and concentrations of naturally occurring tracers can be used to characterize the locations, rates, and sources of baseflow.

Field investigation focused on a 170 km segment of the Little Smoky River, a 75 km segment of the Deep Valley Creek–Simonette river system, and an 85 km segment of the Wildhay–Berland river system. Each river was sampled at several locations (Figure 12) during September 2015, when the rivers were close to their low flow state. Sampling locations span the bedrock formations present in the study area, with the river distance between locations varying from 10 to 40 km, which depended on access to the rivers by roads and trails. Water samples were collected using a peristaltic pump with the intake tubing located on the riverbed and in the middle of the river if possible, otherwise a maximum distance of approximately 3 m from the riverbank. In addition to river water, groundwater was sampled at four locations (Figure 12), including three water wells completed in the Paskapoo Formation (sampled in March 2015) and one well completed in the Wapiti Formation (sampled in November 2015). Each of the water wells had been pumping at the time of sampling, so groundwater was sampled after measurements of temperature, electrical conductivity (EC), and pH appeared stable for the pumping rate at the time of sampling.

The analysis for a suite of naturally occurring environmental tracers allowed for the detection of water of different residence times, identifying young water cycling through the shallow groundwater system and older baseflow sources potentially coming from a deeper groundwater flow system. Each analyte was collected for a different purpose and analyzed by specialized laboratories as described in Table 6.

5.2 Groundwater Discharge Modelling

To estimate the amount of groundwater discharge to the rivers, river flow and the concentration of ^{222}Rn were modelled using coupled mass balance equations for river flow and solute concentration. The approach involves calculating the change in ^{222}Rn in each river, taking into consideration the river flow rate and physical dimensions, and the specific characteristics of ^{222}Rn. This approach to quantifying groundwater discharge to rivers is described by Cook et al. (2006) and has been applied to several river systems to better understand the sources of baseflow (Smerdon et al., 2012a; Harrington et al., 2013; Solomon et al., 2015; Beisner et al., 2018).

For a given river width (w), change in river flow (Q) is expressed as:

$$\frac{\partial Q}{\partial x} = \frac{\partial Q_{tr}}{\partial x} + Pw - Ew + q_{gi}w - q_{go}w \qquad \text{Equation 1}$$

where Q_{tr} is tributary discharge, P is precipitation, E is evaporation, q_{gi} is groundwater gain, q_{go} is groundwater loss, and x is distance. Longitudinal river concentration (c) with distance (x) is expressed as:

$$\frac{\partial C}{\partial x} = \frac{\partial}{\partial x}\left(\frac{DA}{Q}\frac{\partial C}{\partial x}\right) + \frac{q_{gi}w}{Q}C_{gw} - \frac{q_{go}w}{Q}C - \frac{kw}{Q}(C - C_{atm}) - \frac{A}{Q}\lambda C + \frac{1}{Q}\frac{Q_{tr}}{\partial x}C_{tr} \qquad \text{Equation 2}$$

where C is the stream concentration, D is the longitudinal hydrodynamic dispersivity, A is the stream cross-sectional area, C_{gw} is the approximate local groundwater concentration, k is the gas exchange velocity, C_{atm} is the atmospheric equilibrium concentration, λ is the decay coefficient, and C_{tr} is the approximate concentration of the tributary.

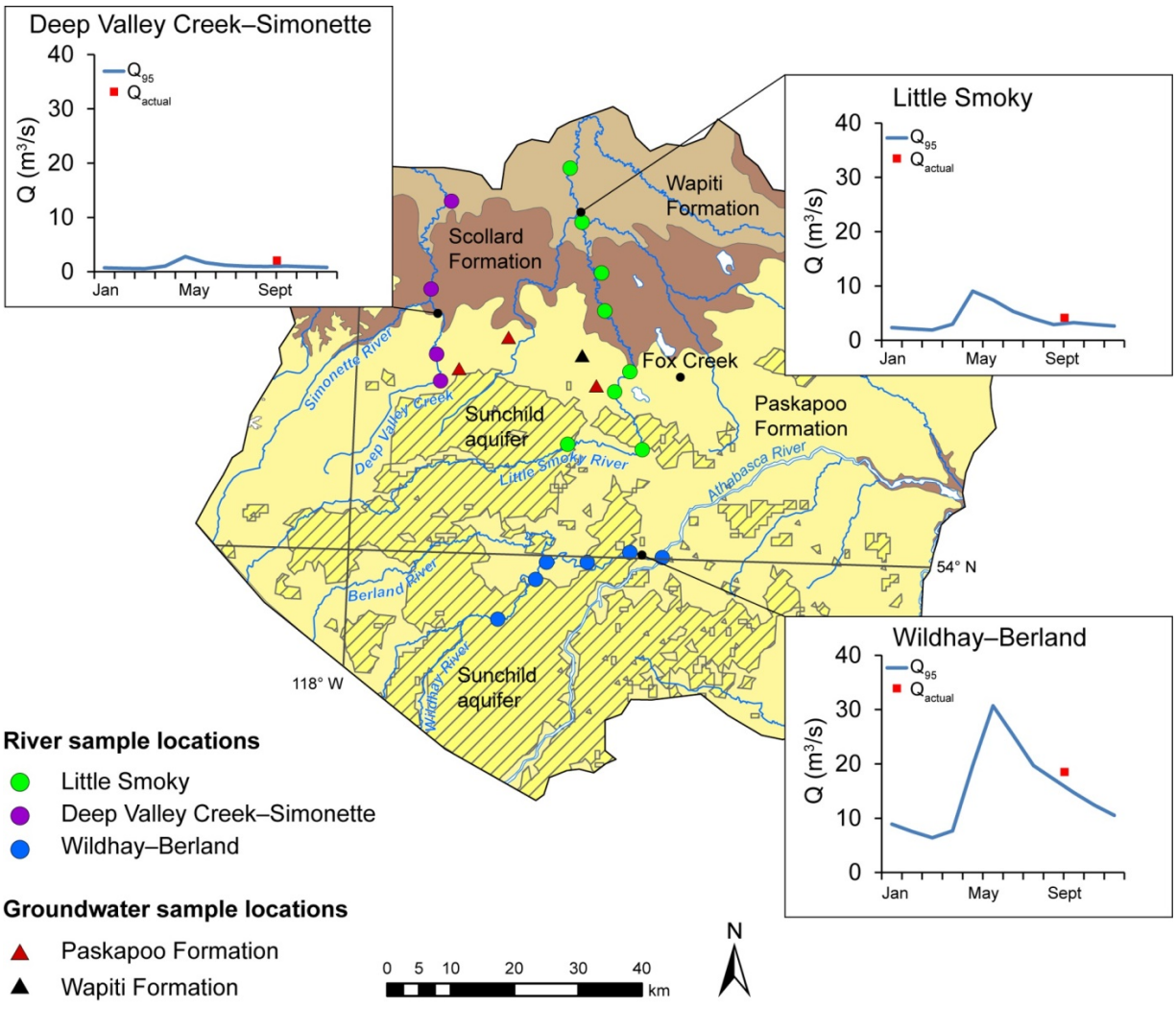

Figure 12. Location of river and groundwater samples relative to bedrock units; Fox Creek area, west-central Alberta. River hydrographs depict the lowest monthly discharge for the period of record (i.e., Q_{95} or the 5th percentile of discharge; Environment and Climate Change Canada, 2018) and the actual discharge (Q_{actual}) at the time of sampling (September 2015). Abbreviation: Q, river discharge.

Table 6. Summary of water sampling and analysts.

Analyte	Purpose	Analyst
Routine water chemistry	Dissolved major ions and alkalinity to understand the general geochemical composition of the water.	Exova Canada Inc. laboratories (Edmonton, Alberta)
Stable isotopes of water ($\delta^{18}O$ and $\delta^{2}H$)	Help understand the origin and movement of the stable isotopes within the hydrological cycle. All values are expressed as δ values representing deviations in per mil (i.e., parts per thousand) from the Vienna standard mean ocean water (VSMOW).	Department of Earth and Atmospheric Sciences at the University of Alberta (Edmonton, Alberta)
Radon-222 (^{222}Rn)	A naturally occurring radioactive gas with an activity that increases in groundwater due to the decay of uranium and radium in geological materials, and rapidly decreases where it equilibrates with the atmosphere. A useful tracer for identifying groundwater discharge to surface water.	Measured on water samples at the end of each day using a RAD7 radon detector (Durridge Company, Inc.)
Sulphur hexafluoride (SF_6)	Present in the atmosphere with concentrations that have increased steadily since the 1960s allowing identification of a modern component in surface water and groundwater (i.e., from recent decades).	Dissolved and Noble Gas Service Center at the University of Utah (Salt Lake City, Utah)
Tritium (^{3}H)	Present in the atmosphere with concentrations that peaked in the 1960s due to atmospheric atomic bomb testing. The decreasing concentration in the atmosphere helps distinguish pre-1960s waters from post-1960s waters.	Dissolved and Noble Gas Service Center at the University of Utah using the helium ingrowth method
Noble gases (Ar, Kr, Xe, Ne, ^{4}He, $^{3}He/^{4}He$ ratio)	Dissolved noble gases in water are used to infer the conditions and time at which precipitation entered the groundwater system.	Dissolved and Noble Gas Service Center at the University of Utah
Radiocarbon (^{14}C)	A radioactive isotope produced in the atmosphere that enters the subsurface through plant respiration. It is an ideal tracer for groundwater movement on the time scale of thousands of years.	Beta Analytic Inc. (Miami, Florida)

Parameters were selected to represent each river system (e.g., depth and width) and the few measured groundwater concentrations determined in this study. For ^{222}Rn, a decay coefficient of 3.82/d was assigned, the atmospheric equilibrium concentration was set to zero, and the gas exchange coefficient was specified using river characteristics and temperature after Raymond et al. (2012).

Equations 1 and 2 are coupled through the river discharge and geometry of the river, and were solved numerically using the method described by Beisner et al. (2018). Average groundwater discharge to the rivers was estimated by fitting Equation 2 to the measured concentrations of ^{222}Rn using a Marquart-Levenberg optimization routine, which minimized the chi-squared residual between modelled and observed ^{222}Rn and river flow.

5.3 Geochemical and Isotopic Results

All geochemical and isotopic results are tabulated in Appendix 1. The results presented and discussed in this section focus on the circulation of groundwater in the study area and its interaction with surface water.

River water samples were found to have TDS values less than 250 mg/L, with a distinct difference between each river system. The TDS values varied from 161to 192 mg/L for the Little Smoky River, from 180 to 220 mg/L for the Deep Valley Creek–Simonette river system, and from 228 to 248 mg/L for the Wildhay–Berland river system (Figure 13). Although subtle, there was a consistent increase of TDS in the downstream direction for the Little Smoky and Deep Valley Creek–Simonette river systems, and a decrease in the downstream direction for the Wildhay–Berland river system (Figure 14a). Groundwater

from three samples in the Paskapoo Formation were found to have TDS values varying from 378 to 506 mg/L, consistent with the results from regional data sources shown on Figure 9. The single groundwater sample from the Wapiti Formation had a value of 1740 mg/L, similar to the few other measurements in this region mapped by Nakevska and Singh (2019).

Radon activity in the rivers was found to vary from 0.05 to 0.32 becquerel per litre (Bq/L), with most values close to the average of 0.17 Bq/L. In groundwater samples from the Paskapoo Formation, radon activity varied from 7.6 to 25.1 Bq/L. Similar to TDS, ^{222}Rn was found to be higher for the Deep Valley Creek–Simonette and Wildhay–Berland river systems than the Little Smoky River (Figure 13). The spatial variation appears to be somewhat related to the sandstone abundance of the uppermost 50 m of bedrock (Figure 13) and provides an indication to the amount of groundwater discharge to these rivers that will be discussed further in Section 5.4.

The results for stable isotopes of water are shown on Figure 15 relative to local meteoric water lines (LMWLs) developed for the Utikuma Region Study Area (URSA), which is located 225 km northeast of the study area (Smerdon et al., 2012b), and Edmonton, which is located 260 km southeast of the study area (Maulé et al., 1994). River water plots on the lower part of the LMWL for rainfall at URSA, with values for the Wildhay–Berland and Deep Valley Creek–Simonette river systems clustering more closely together than the Little Smoky River. Groundwater from the Paskapoo Formation plots at the transition between rainfall and snow segments of the URSA LMWL, confirming the broadly held understanding that the majority of groundwater is recharged from snowmelt (Jasechko et al., 2014), especially in west-central Alberta (Smerdon et al., 2008). The stable isotope results provide an indication that the Wildhay–Berland and Deep Valley Creek–Simonette river systems are better connected to groundwater than the Little Smoky River.

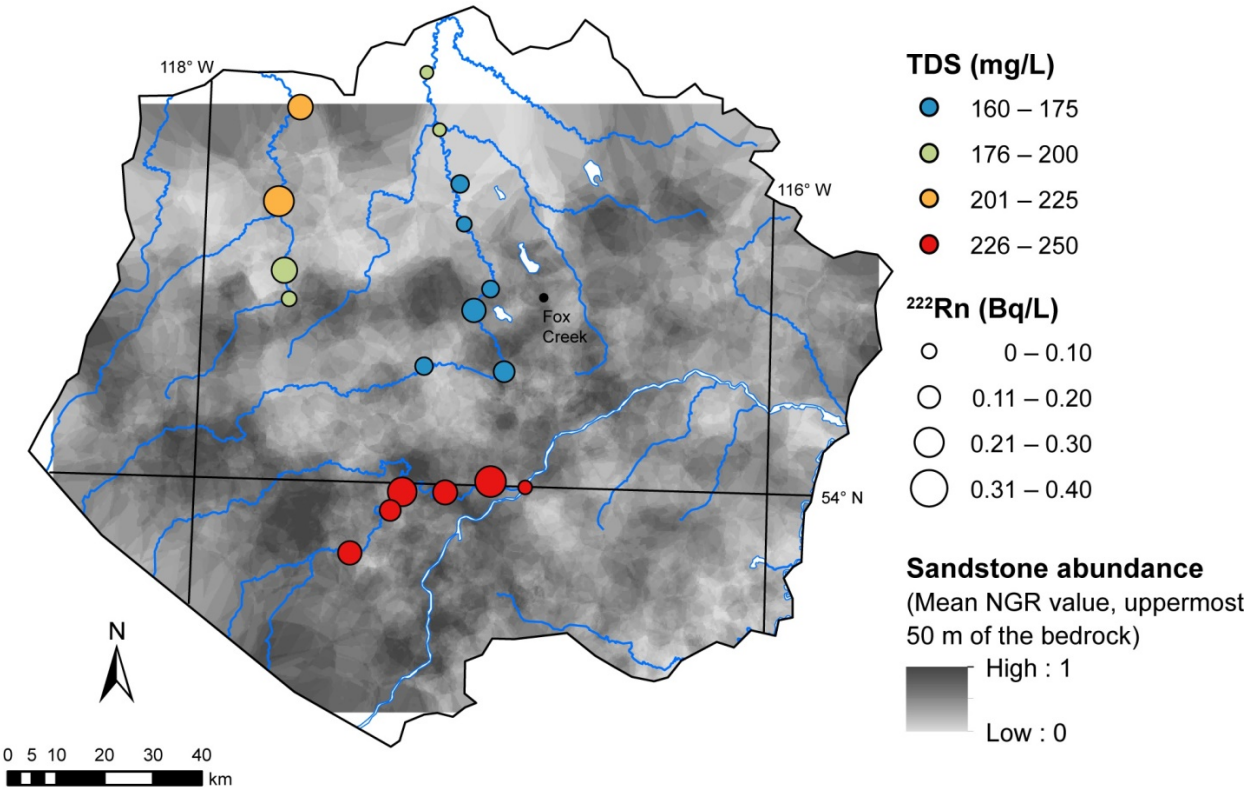

Figure 13. Summary of total dissolved solids (TDS) and ^{222}Rn concentrations in river water shown with abundance of sandstone in the uppermost 50 m of the bedrock formations, Fox Creek area, west-central Alberta. Abbreviations: Bq, becquerel; NGR, net-to-gross ratio.

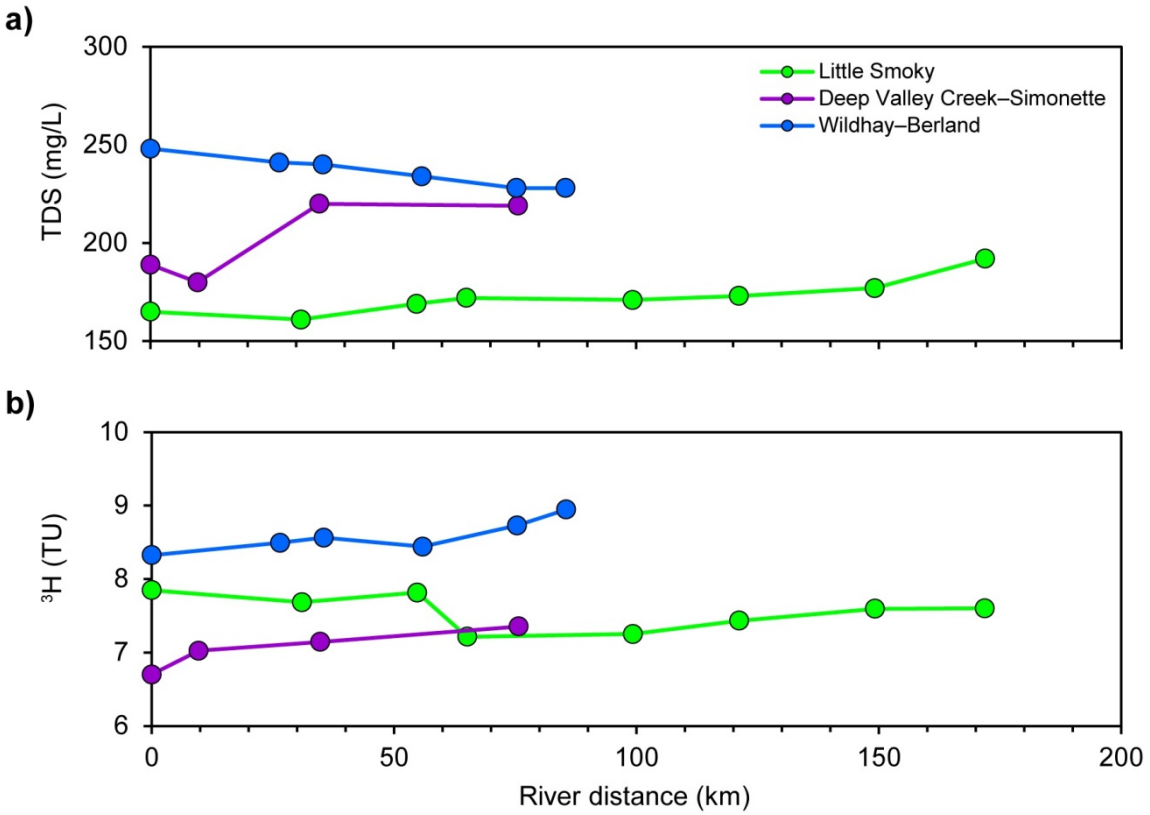

Figure 14. a) Total dissolved solids (TDS) and b) ^{3}H concentrations in river water plotted as distance along sampled segments of each river / river system in Fox Creek area, west-central Alberta. Abbreviation: TU, tritium unit.

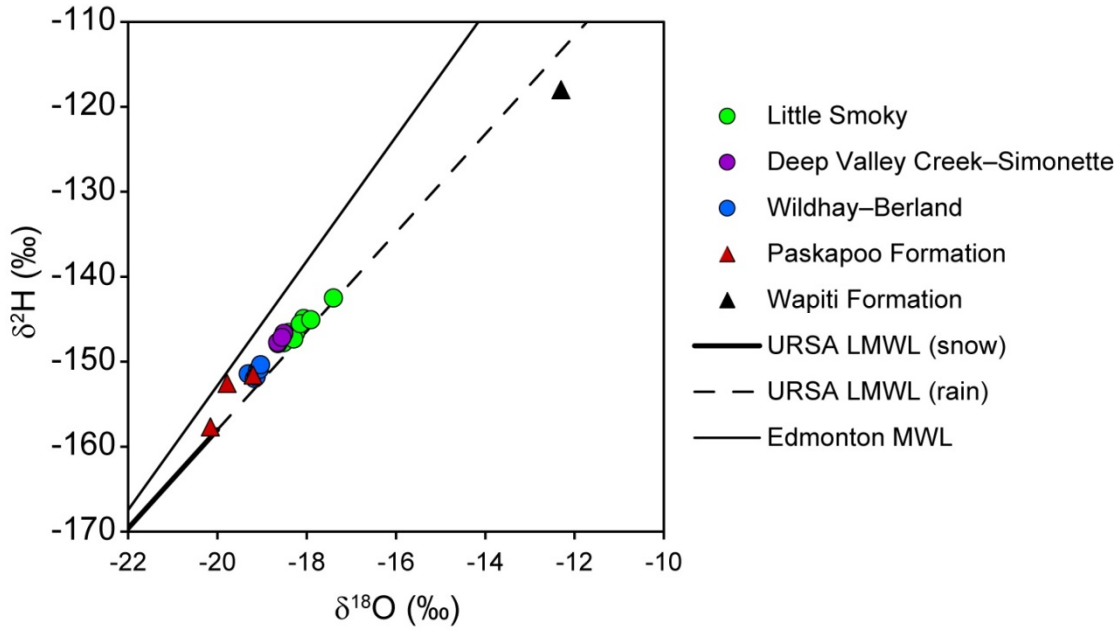

Figure 15. Stable isotope values (δ^2H and δ^{18}O) for river and groundwater samples (from the Fox Creek area in west-central Alberta) relative to Local Meteoric Water Line (LMWL) from the Utikuma Research Study Area (URSA) reported in Smerdon et al. (2012b) and Meteoric Water Line (MWL) for Edmonton by Maulé et al. (1994).

The atmospheric concentrations of ^{3}H and SF_6 since the 1960s (Figure 16a) help determine the presence of relatively young water in the groundwater cycle. In the study area, the values for ^{3}H range from 6.7 to 9.0 tritium units (TU) and were found to be distinct for each river system, similar to TDS values (Figure 14b). When the results of ^{3}H and SF_6 are plotted together (Figure 16b), it can be seen that the rivers contain water representative of the 2008 to 2012 period. However, groundwater from the Paskapoo Formation was found to have both low ^{3}H (0.1 to 4.5 TU) and SF_6 (0.007 to 0.073 picogram/kg) values, suggesting a residence time greater than 50 years. The groundwater sample from the Wapiti Formation had only 0.05 TU (±0.02 TU error) indicating a residence time much greater than 50 years, and was not analyzed for SF_6.

In this study, noble gas concentrations and radiocarbon were used to identify older water in the groundwater cycle. Helium-4 is a nonradioactive noble gas that accumulates slowly in groundwater due to the decay of uranium in geological materials, making it a suitable tracer for groundwater with a residence time of greater than 1000 years. The concentration of ^{4}He was found to be in the order of 4×10^{-8} cubic centimetres, at standard temperature and pressure, per gram (ccSTP/g) for the river samples (Figure 17a), and higher for groundwater from the Paskapoo (6×10^{-8} to 2×10^{-7} ccSTP/g) and Wapiti formations (2×10^{-6} ccSTP/g). Estimating the residence time from ^{4}He concentration requires knowing additional details about the production rate for each specific rock type, transfer from the rock to aqueous phase, and the evolution of these factors along a groundwater flow path. However, if an average production rate of ^{4}He from geological materials is assumed, the concentrations found for the Paskapoo Formation samples would correspond to a residence time of 1000 to 10 000 years, and more than 100 000 years for the sample from the Wapiti Formation. Although the ^{14}C data have not been plotted, the groundwater sample from the Wapiti Formation was found to contain only 0.9 percent of modern carbon, which is effectively zero and confirms a residence time greater than 30 000 years.

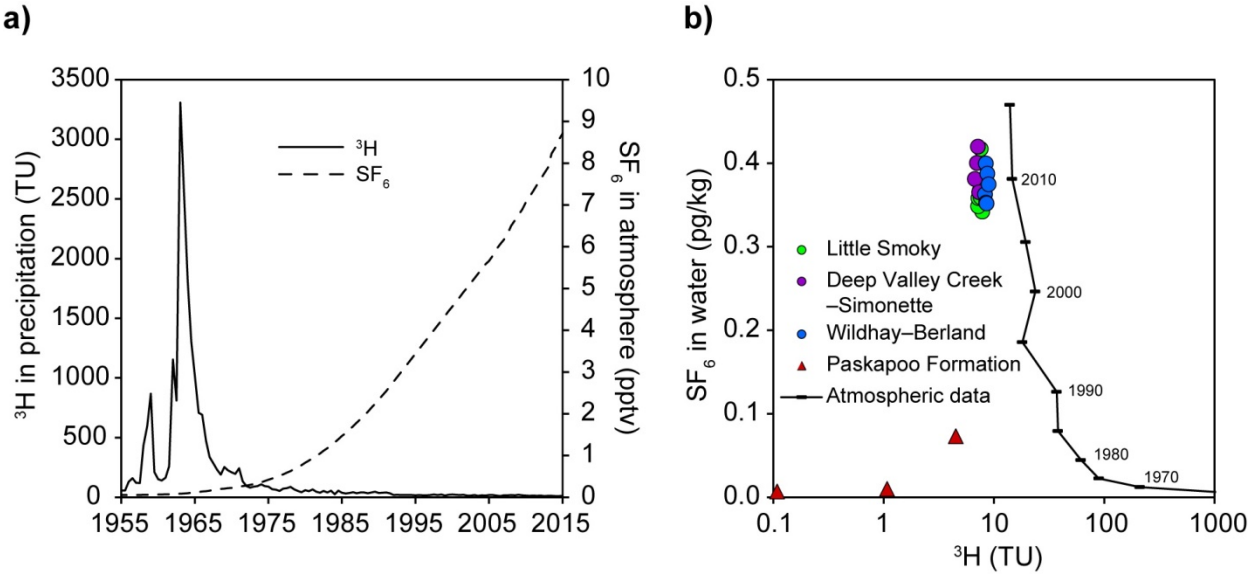

Figure 16. a) Historical atmospheric concentrations of ^{3}H measured in Ottawa, Ontario, and SF_6 measured in Niwot Ridge, Colorado. b) The ^{3}H and SF_6 results for river and groundwater samples (from the Fox Creek area, west-central Alberta) plotted with five year average atmospheric concentrations from a). Abbreviations: pg, picogram; pptv, parts per trillion by volume; TU, tritium units.

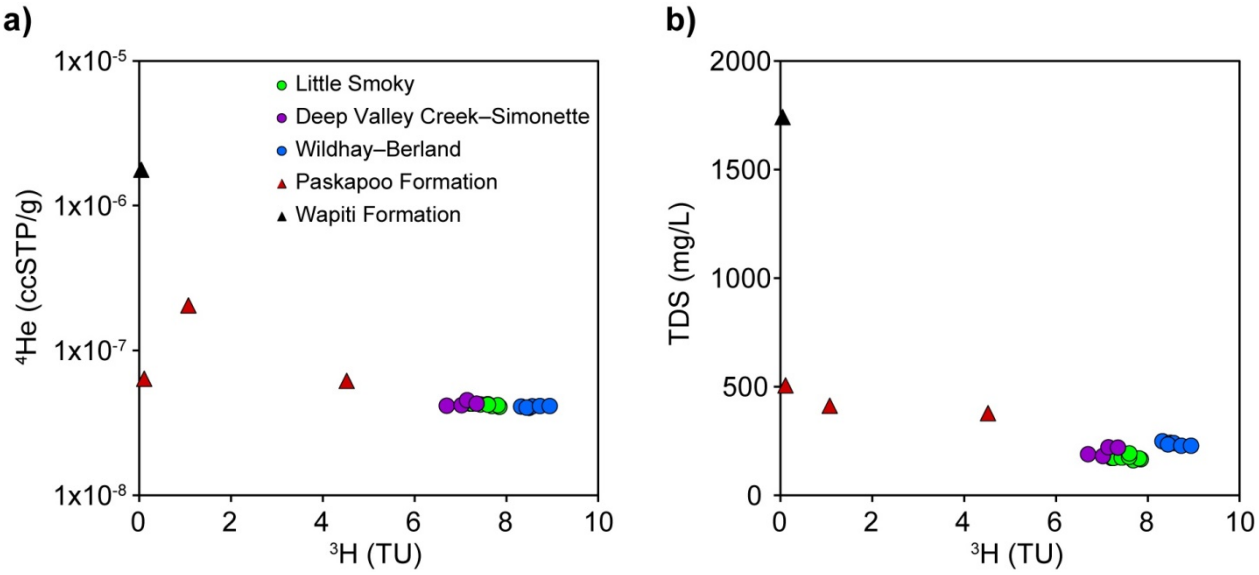

Figure 17. Environmental tracer results illustrating the mixing of young water (^{3}H) and older waters having increased concentrations of a) ^{4}He and b) total dissolved solids (TDS). River and groundwater samples from the Fox Creek area, west-central Alberta. Abbreviations: ccSTP, cubic centimetres at standard temperature and pressure; TU, tritium units.

5.4 Spatial Variation in Baseflow

The groundwater discharge modelling described in Section 5.2 is intended to provide insight into the potential variation in groundwater discharge, which provides baseflow to each of the rivers sampled. Figure 18 illustrates the resultant groundwater discharge required to match the measured concentration of ^{222}Rn and river flow in each of the river systems. For context, the actual river flow (Q_{actual}) at the time of sampling is shown with the long-term low flow (Q_{95}) for the month of September. Each subsection of Figure 18 contains the measured and modelled profiles of ^{222}Rn and river discharge at the time of sampling, as well as the modelled profile of groundwater inflow to the river.

For the Little Smoky River (Figure 18a), groundwater inflow was generally low, with the majority (7.3×10^{-6} m^3/s) occurring within the first 50 km of the sampled river. This portion of the river coincides with the Sunchild aquifer and the northern margin of the Paskapoo Formation (Figure 12). For the Deep Valley Creek–Simonette river system (Figure 18b), groundwater discharge decreased from a high of 7.2×10^{-6} m^3/s to effectively zero by 25 km. This portion of the river coincides with the northern margin of the Paskapoo Formation (Figure 12). For the Wildhay–Berland river system (Figure 18c), groundwater discharge increased along the distance sampled, to a maximum of 9.3×10^{-6} m^3/s in the vicinity of the Sunchild aquifer near the Athabasca River (Figure 12).

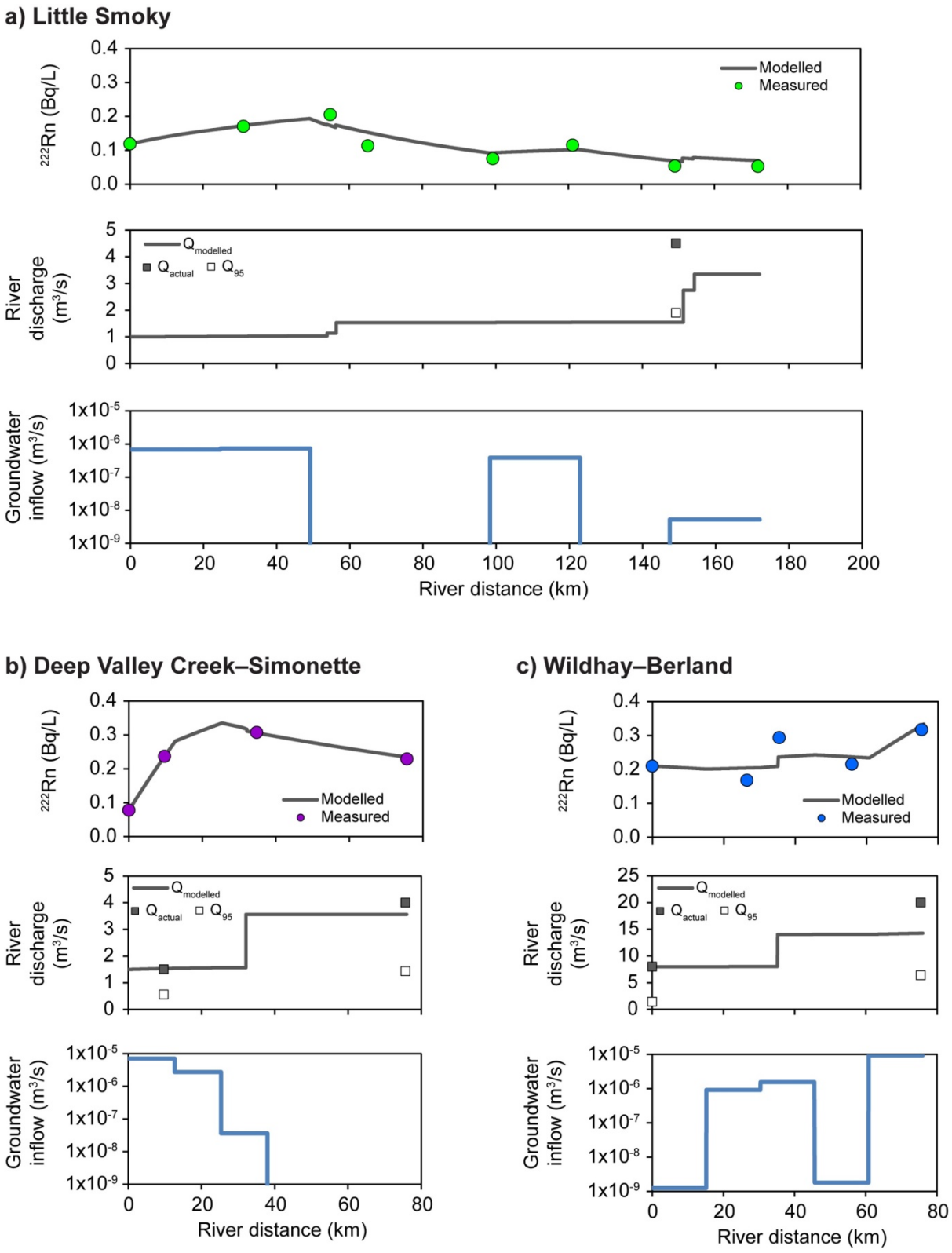

Figure 18. Measured and modelled concentration of ^{222}Rn in the river water samples and the resultant modelled rate of groundwater inflow for each river / river system. Measured in September 2015, Fox Creek area, west-central Alberta. Abbreviations: Q_{95}, 5th percentile of river flow; Q_{actual}, actual river flow; $Q_{modelled}$, modelled river flow.

6 Nonsaline Groundwater Circulation

Groundwater circulation from recharge areas to discharge areas is largely controlled by the hydrostratigraphic framework described in Section 2.3 and the corresponding hydraulic pathways illustrated in Figure 11. Interaction with more saline groundwater (i.e., >4000 mg/L) occurs within deeper portions of the Wapiti Formation; however, the focus of the current study is groundwater movement and interaction with surface water, which is typically nonsaline. Figure 19 brings together key elements of the hydrostratigraphic framework and groundwater flow patterns to summarize groundwater circulation and interaction with surface water in the Fox Creek area. On Figure 19a, regional hydraulic pathways 1 and 2 (Figure 11d) have been combined to delineate potential recharge areas, and the results of groundwater inflow modelling have been portrayed spatially to define potential discharge areas.

In the southwestern portion of the study area, relatively high precipitation, elevated topography, and the presence of regional hydraulic pathways create favourable conditions for groundwater recharge. The abundance of sandstone in the uppermost bedrock promotes groundwater circulation to a depth greater than would be expected in the northern portion of the study area, where precipitation is lower and regional hydraulic pathways are less likely. The abundance of sandstone in the southwestern portion of the study area also influences the rate of groundwater discharge. Firstly, the deeply incised channels create a convergence of groundwater flow from the benchland areas towards rivers, as illustrated for the Wildhay–Berland river system and the segment of the Little Smoky River where the river course shifts from eastward to northward flow in the centre of the study area (Figure 19). Secondly, the sandstone has higher hydraulic conductivity compared to more mudstone-dominated sections of the Paskapoo Formation, which promotes a greater volume of groundwater discharge to rivers. For both the Wildhay–Berland river system and upper segment of the Little Smoky River, the source of baseflow is a combination of young groundwater that has recharged relatively close to the rivers, and much older groundwater that has recharged from upgradient locations and circulated deeper within the sandstone-rich zones within the bedrock. This mixture of waters discharging to rivers likely has a mean age of a few hundred years.

In the northern portion of the study area, less precipitation and a more subdued plains landscape create less opportunity for groundwater recharge to circulate to local river systems. The Deep Valley Creek–Simonette river system and the Little Smoky River both traverse the northern part of the Paskapoo Formation, and across the subcrop areas of the Scollard and upper Wapiti formations. In this part of the study area, the Paleogene–Quaternary units and uppermost bedrock units have lower hydraulic conductivity, thereby limiting the amount of groundwater discharge to the rivers. The rate of groundwater inflow decreases as the rivers flow northwards, and the source of baseflow shifts to young groundwater, which likely has a mean age of about a decade. However, a deeper component of groundwater flow is present in the Wapiti Formation that likely does not interact with surface water in the study area. North of the study area, the more permeable parts of the Wapiti Formation (e.g., basal sandstone aquifer shown on Figure 4b) subcrop and could receive modern recharge and interact with surface water.

The conceptual movement of nonsaline groundwater in the Fox Creek area can be summarized through two hydrogeological landscapes, as illustrated in Figure 20. For each hydrogeological landscape, the source of groundwater recharge is dominantly snowmelt. Where there is high topographic relief, the bedrock is generally close to ground surface and comprises abundant sandstone bodies that promote deep circulation of groundwater that discharges to local rivers within a few hundred years (Figure 20a). Where there is low topographic relief, the bedrock may be deeper and dominated by mudstone. In these locations, groundwater recharge is minimized and local rivers capture adjacent groundwater within a decade (Figure 20b). These hydrogeological landscapes provide context to evaluate both surface and groundwater in the Fox Creek area, and offer a conceptual model to further develop quantitative water balance tools.

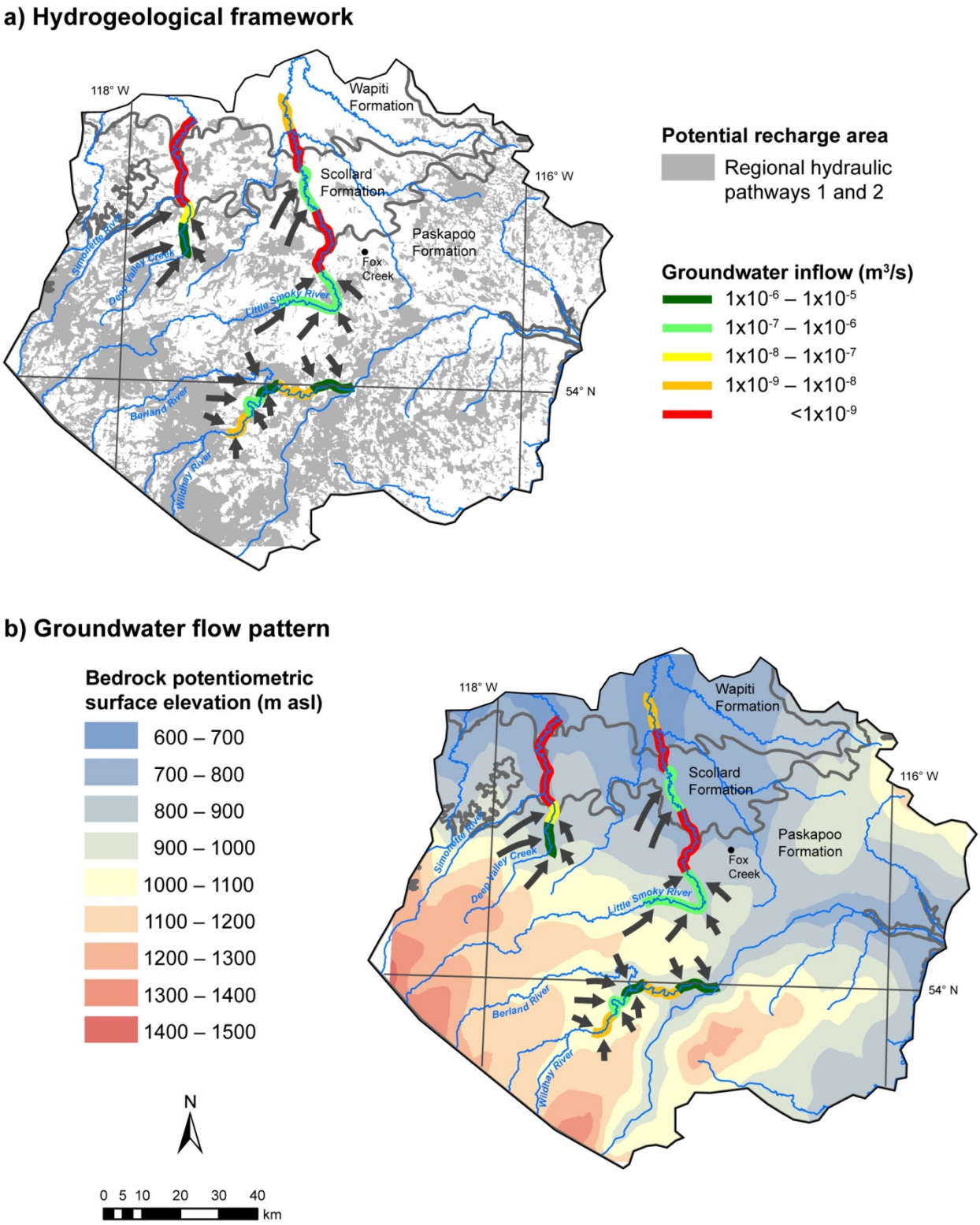

Figure 19. Modelled groundwater inflow for each river compared to a) regional hydraulic pathways having a high likelihood of vertical groundwater movement (Figure 11d); and b) potentiometric surface for the uppermost bedrock units (Figure 6), Fox Creek area, west-central Alberta. Arrows indicate the groundwater flow pathways supporting each river system. The size of the arrow indicates the relative magnitude of groundwater flow.

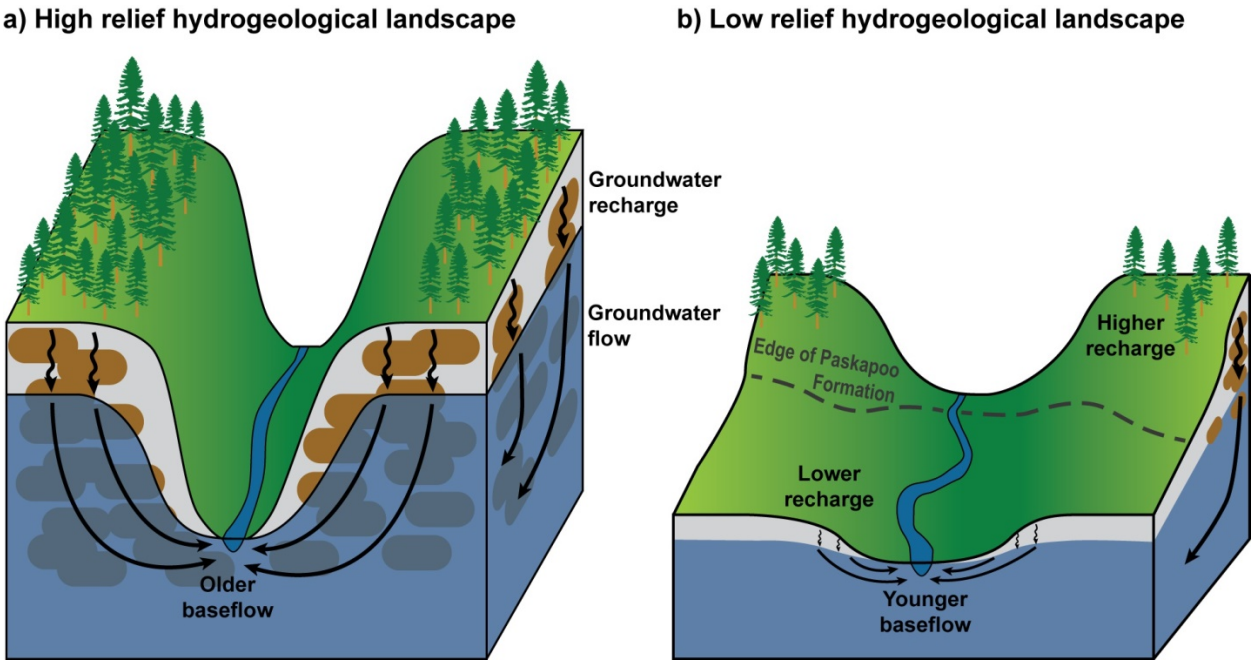

Figure 20. Conceptual hydrogeological landscapes for the Fox Creek area, west-central Alberta: a) high relief landscapes characterized by numerous sand(stone) bodies (brown) generating deep groundwater circulation and older baseflow to rivers; and b) low relief landscapes in mud-dominated geological settings generating localized groundwater recharge and younger baseflow to rivers.

7 Summary and Future Work

In west-central Alberta the co-location of several industries exerts pressure on land and water resources, including oil and gas development, forestry, and agriculture. Knowledge of the Upper Cretaceous–Quaternary hydrological system is needed to support regulation decisions and assessment of the cumulative effects of these activities. This report brings together geological modelling with an assessment of groundwater conditions to develop a conceptual understanding of the hydrogeological framework, circulation of groundwater, and interaction with surface water in the Fox Creek area. Previous modelling of Paleogene–Quaternary sediments and bedrock units is integrated to define regional hydraulic pathways that identify locations where enhanced vertical groundwater movement can be expected. Groundwater data, including chemistry and hydraulic head information, confirm the generally accepted understanding of a dominance of groundwater recharge across the study area where the Paskapoo Formation is present. Additional data acquired as part of this study, indicates that groundwater recharge is sourced primarily from snowmelt and that there is large spatial variation in groundwater discharge to river systems. Circulation of groundwater is summarized by two conceptual hydrogeological landscapes, generally based on topographic relief. Where sandstone is abundant, relief typically is high and results in deeper groundwater circulation and older baseflow sources to local rivers. Where relief is lower, sediments and bedrock of lower hydraulic conductivity typically limit groundwater recharge, resulting in more localized groundwater capture to rivers and younger baseflow sources.

The hydrogeological characterization developed for the Fox Creek area is sufficient to support regulation decisions and assessment of cumulative effects, through a better understanding of the nonsaline hydrological system, which can be incorporated into quantitative tools such as numerical models and decision support systems.

This study recognized that future geoscience work should be focused on refining the geological and hydrogeological characterization of the Wapiti Formation and expanding knowledge of groundwater chemistry. The Wapiti Formation contains a thick basal sandstone unit and several intervening layers that will be important from a hydrogeological perspective, especially north and northwest of the study area, where the Wapiti Formation is shallower, and likely more active in nonsaline groundwater circulation. Strategic groundwater sampling within the study area, and towards the northwest, will confirm some of the groundwater-age relationships learned from sampling rivers in the current study.

8 References

Alberta Energy Regulator (2019): Alberta water use performance report; URL <https://www2.aer.ca/t/Production/views/AlbertaWaterUseReport_0/WaterSummary?:embed=y&:display_count=no&:showShareOptions=true&:showVizHome=no> [May 2019].

Alberta Environment and Parks (2018): Alberta Water Well Information Database; URL <https://www.alberta.ca/alberta-water-well-information-database-overview.aspx> [May 2019].

Atkinson, L.A. and Hartman, G.M.D. (2017): 3D rendering of the regional stratigraphy of Paleogene-Quaternary sediments in west-central Alberta; Alberta Energy Regulator, AER/AGS Report 93, 44 p., URL <http://ags.aer.ca/document/REP/REP_93.pdf> [May 2019].

Babakhani, M. and MacCormack, K. (2019): 3D geological model of west–central Alberta – methodology and metadata; in 3D geological model of west-central Alberta, Alberta Energy Regulator / Alberta Geological Survey, AER/AGS Model 2019-03, 62 p., URL <https://ags.aer.ca/publications/MOD_2019_03.html> [August 2019].

Babakhani, M., Mei, S., Atkinson, L.A. and Smerdon, B.D. (2019): 3D property modelling of the bedrock hydrostratigraphy in the Fox Creek area, west-central Alberta; Alberta Energy Regulator / Alberta Geological Survey, AER/AGS Open File Report 2019-03, 19 p., URL <https://ags.aer.ca/publications/OFR_2019_03.html> [August 2019].

Beisner, K.R., Gardner, W.P. and Hunt, A.G. (2018): Geochemical characterization and modeling of regional groundwater contributing to the Verde River, Arizona between Mormon Pocket and the USGS Clarkdale gage; Journal of Hydrology, v. 564, p. 99–114, doi:10.1016/j.jhydrol.2018.06.078

Cook, P.G., Lamontagne, S., Berhane, D. and Clark, J.F. (2006): Quantifying groundwater discharge to Cockburn River, southeastern Australia, using dissolved gas tracers ^{222}Rn and SF_6; Water Resources Research, v. 42, W10411, doi:10.1029/2006WR004921

Corlett, H.J., Playter, T.L., Babakhani, M., Hathway, B., Peterson, J.T. and MacCormack, K.E. (2019): Regional stratigraphic correlation and 3D geological modelling of west-central Alberta; Alberta Energy Regulator / Alberta Geological Survey, AER/AGS Open File Report 2019-04, 53 p., URL <https://ags.aer.ca/publications/OFR_2019_04.html> [August 2019].

Dawson, F.M., Kalkreuth, W.D. and Sweet, A.R. (1994): Stratigraphic and coal resource potential of the Upper Cretaceous to Tertiary strata of northwestern Alberta; Geological Survey of Canada, Bulletin 466, 67 p.

Demchuk, T.D. and Hills, L. (1991): A re-examination of the Paskapoo Formation in the central Alberta Plains: the designation of three new members; Bulletin of Canadian Petroleum Geology, v. 39, no. 3, p. 270–282, URL <http://archives.datapages.com/data/cspg/data/039/039003/0270.htm> [May 2019].

Environment and Climate Change Canada (2018): HYDAT database; Environment and Climate Change Canada, URL <https://ec.gc.ca/rhc-wsc/default.asp?lang=En&n=9018B5EC-1> [May 2019].

Fanti, F. and Catuneanu, O. (2009): Stratigraphy of the Upper Cretaceous Wapiti Formation, west-central Alberta, Canada; Canadian Journal of Earth Sciences, v. 46, no. 4, p. 263–286, doi:10.1139/E09-020

Grasby, S., Tan, W., Chen, Z. and Hamblin, A.P. (2007): Paskapoo groundwater study part I: hydrogeological properties of the Paskapoo Formation determined from six continuous cores; Geological Survey of Canada, Open File 5392, 6 p., doi:10.4095/223756

Grasby, S.E., Chen, Z., Hamblin, A.P., Wozniak, P.R.J. and Sweet, A.R. (2008): Regional characterization of the Paskapoo bedrock aquifer system, southern Alberta; Canadian Journal of Earth Sciences, v. 45, no. 12, p. 1501–1516, doi:10.1139/E08-069

Hamblin, A.P. (2004): Paskapoo-Porcupine Hills formations in western Alberta: synthesis of regional geology and resource potential; Geological Survey of Canada, Open File 4679, 30 p.

Harrington, G.A., Payton, Gardner W. and Munday, T.J. (2013): Tracking groundwater discharge to a large river using tracers and geophysics; Groundwater, v. 52, no. 6, p. 837–852, doi:10.1111/gwat.12124

Hathway, B. (2011): Tops of the Horseshoe Canyon, Wapiti and Battle formations in the west-central Alberta Plains: subsurface stratigraphic picks and modelled surface; Energy Resources Conservation Board, ERCB/AGS Open File Report 2011-08, 24 p., URL <http://ags.aer.ca/publications/OFR_2011_08.html> [May 2019].

Hughes, A.T., Smerdon, B.D. and Alessi, D.S. (2017a): Hydraulic properties of the Paskapoo Formation in west-central Alberta; Canadian Journal of Earth Sciences, v. 54, no. 8, p. 883–892, doi:10.1139/cjes-2016-0164

Hughes, A.T., Smerdon, B.D. and Alessi, D.S. (2017b): A summary of hydraulic conductivity values for the Paskapoo Formation in west-central Alberta; Alberta Energy Regulator, AER/AGS Open File Report 2016-03, 25 p., URL <http://ags.aer.ca/publications/OFR_2016_03.html> [May 2019].

IHS Markit (2018): AccuMap™; IHS Markit, mapping, data management and analysis software, URL <https://ihsmarkit.com/products/oil-gas-tools-accumap.html> [May 2019].

Irish, E.J.W. (1970): The Edmonton Group of south-central Alberta; Bulletin of Canadian Petroleum Geology, v. 18, no. 2, p. 125–155.

Jasechko, S., Birks, S.J., Gleeson, T., Wada, Y., Fawcett, P.J., Sharp, Z.D., McDonnell, J.J. and Welker, J.M. (2014): The pronounced seasonality of global groundwater recharge; Water Resources Research, v. 50, p. 8845–8867, doi:10.1002/2014WR015809

Lyster, S. and Andriashek, L.D. (2012): Geostatistical rendering of the architecture of hydrostratigraphic units within the Paskapoo Formation, central Alberta; Energy Resources Conservation Board, ERCB/AGS Bulletin 66, 115 p., URL <http://ags.aer.ca/publications/BUL_066.html> [May 2019].

Klassen, J. and Smerdon, B.D. (2018): First-order groundwater availability assessment for central Alberta; Alberta Energy Regulator, AER/AGS Open File Report 2017-07, 28 p., URL <https://ags.aer.ca/publications/OFR_2017_07.html> [May 2019].

Maulé, C.P., Chanasyk, D.S. and Muehlenbachs, K. (1994): Isotopic determination of snow-water contribution to soil water and groundwater; Journal of Hydrology, v. 155, no. 1–2, p. 73–91, doi:10.1016/0022-1694(94)90159-7

Mwale, D., Gan, T.Y., Devito, K., Mendoza, C., Silins, U. and Petrone, R. (2009): Precipitation variability and its relationship to hydrologic variability in Alberta; Hydrological Processes, v. 23, no. 21, p. 3040–3056, doi:10.1002/hyp.7415

Nakevska, N. and Singh, A. (2019): Distribution of total dissolved solids in the Wapiti / Belly River hydrostratigraphic unit; Alberta Energy Regulator, AER/AGS Map 542, scale 1:1 750 000, URL <https://ags.aer.ca/publications/MAP_542.html> [May 2019].

Pettapiece, W.W. (1986): Physiographic subdivisions of Alberta; Agriculture Canada, Research Branch, Land Resource Research Centre, scale 1:1 500 000.

Quartero, E.M., Leier, A.L., Bentley, L.R. and Glombick, P. (2015): Basin-scale stratigraphic architecture and potential Paleocene distributive fluvial systems of the Cordilleran Foreland Basin, Alberta, Canada; Sedimentary Geology, v. 316, p. 26–38, doi:10.1016/j.sedgeo.2014.11.005

Raymond, P.A., Zappa, C.J., Butman, D., Bott, T.L., Potter, J., Mulholland, P., Laursen, A.E., McDowell, W.H. and Newbold, D. (2012): Scaling the gas transfer velocity and hydraulic geometry in streams

and small rivers; Limnology and Oceanography: Fluids and Environments, v. 2, no. 1, p. 41–53, doi:10.1215/21573689-1597669

Smerdon, B.D., Mendoza, C.A. and Devito, K.J. (2008): Influence of subhumid climate and water table depth on groundwater recharge in shallow outwash aquifers; Water Resources Research, v. 44, W08427, doi:10.1029/2007WR005950

Smerdon, B.D., Gardner, W.P., Harrington, G.A. and Tickell, S.J. (2012a): Identifying the contribution of regional groundwater to the baseflow of a tropical river (Daly River, Australia); Journal of Hydrology, v. 464–465, p. 107–115, doi:10.1016/j.jhydrol.2012.06.058

Smerdon, B.D., Mendoza, C.A. and Devito, K.J. (2012b): The impact of gravel extraction on groundwater dependent wetlands and lakes in the Boreal Plains, Canada; Environmental Earth Sciences, v. 67, no. 5, p. 1249–1259, doi:10.1007/s12665-012-1568-4

Smerdon, B.D., Atkinson, L.A., Hartman, G.M.D., Playter, T.L. and Andriashek, L.D. (2016): Field evidence of nested groundwater flow along the Little Smoky River, west-central Alberta; Alberta Energy Regulator, AER/AGS Open File Report 2016-02, 34 p., URL <http://ags.aer.ca/publications/OFR_2016_02.html> [May 2019].

Solomon, D.K., Gilmore, T.E., Solder, J.E., Kimball, B. and Genereux, D.P. (2015): Evaluating an unconfined aquifer by analysis of age-dating tracers in stream water; Water Resources Research, v. 51, no. 11, p. 8883–8899, doi:10.1002/2015WR017602

Wang, T., Hamann, A., Spittlehouse, D. and Carroll, C. (2016): Locally downscaled and spatially customizable climate data for historical and future periods for North America; PLoS ONE, v. 11, no. 6, e0156720.

Appendix 1 – Geochemical and Isotopic Data

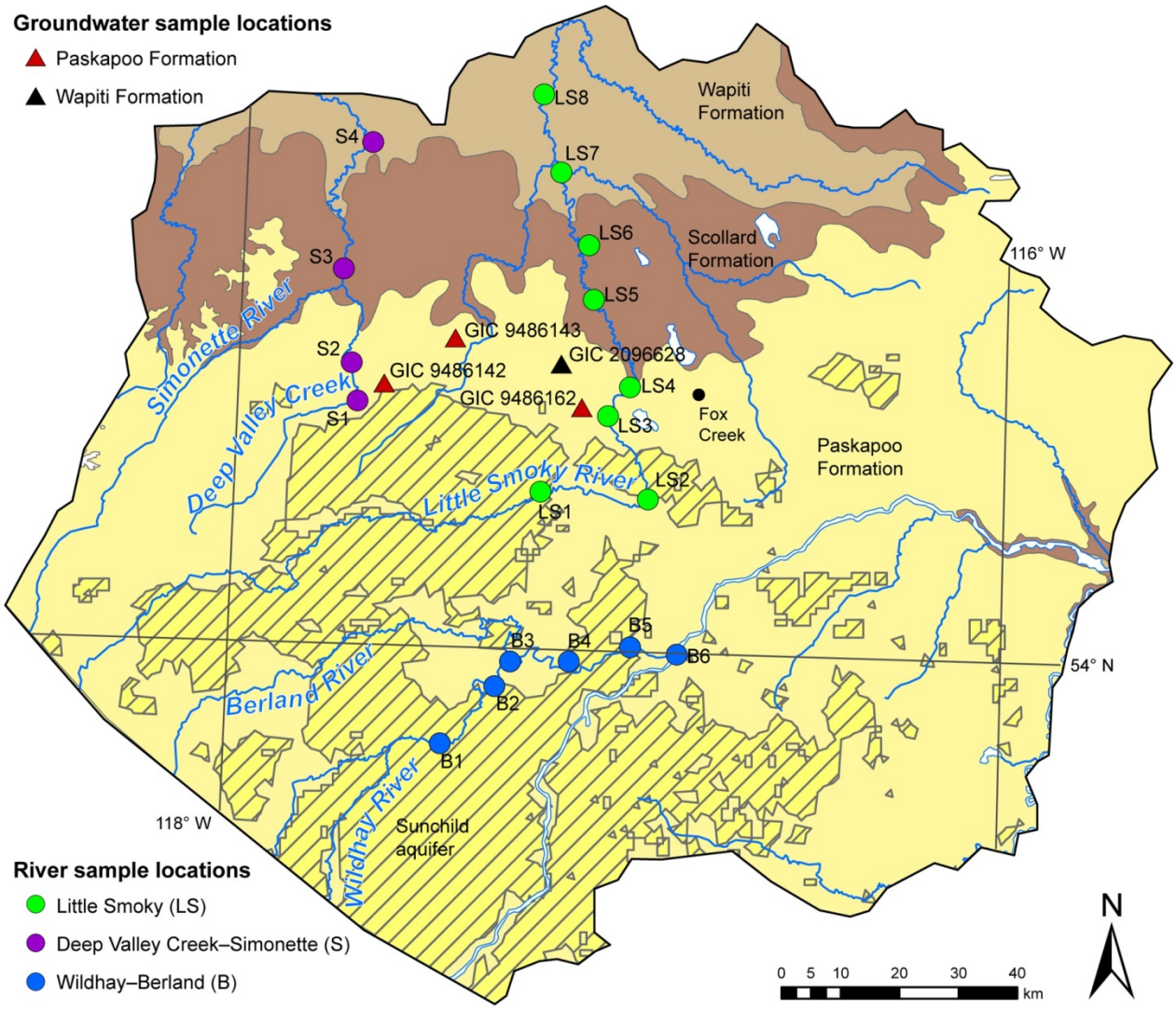

Figure 21. Location of river and groundwater samples, Fox Creek area, west-central Alberta.

Table 7. Location of river and groundwater samples, Fox Creek area, west-central Alberta.

Location	Sample ID	Latitude	Longitude	GPS Elevation (m asl)	Notes
Little Smoky River	LS1	54.24643	-117.20952	953.8	
	LS2	54.23927	-116.92989	863.0	
	LS3	54.36488	-117.04013	787.9	
	LS4	54.40914	-116.98417	773.4	
	LS5	54.54139	-117.08509	721.3	
	LS6	54.62393	-117.10201	694.9	
	LS7	54.73384	-117.18169	661.3	
	LS8	54.85168	-117.23369	627.4	
Deep Valley Creek – Simonette river system	S1	54.37530	-117.69508	870.6	
	S2	54.43389	-117.71364	824.3	
	S3	54.57602	-117.74403	737.0	
	S4	54.77019	-117.67966	590.0	
Wildhay–Berland river system	B1	53.85821	-117.44898	1009.4	
	B2	53.94791	-117.31332	953.2	
	B3	53.98640	-117.27491	946.4	
	B4	53.98884	-117.12234	880.6	
	B5	54.01349	-116.96574	868.0	
	B6	54.00399	-116.84391	821.4	
Paskapoo Formation groundwater					
06-29-063-23W5M[a]	GIC 9486143	54.47708	-117.44421	870	Screened from 24.4–41.2 m
08-35-062-25W5M	GIC 9486142	54.40412	-117.62676	910	Screened from 21.3–36.3 m
07-20-062-21W5M	GIC 9486162	54.37715	-117.10848	880	Screened from 14.9–24.4 m
Wapiti Formation groundwater					
05-18-063-21W5M	GIC 2096628	54.448907	-117.17393	844	Screened from 968.1–1006.1 m

[a] Abbreviated form of L.S. 6, Sec. 29, Twp. 63, Rge. 23, W 5th Mer.

Table 8. Field measured parameters, radon activity, and stable isotopic ratios of river and groundwater samples, Fox Creek area, west-central Alberta.

Sample ID	Temperature (°C)	pH	Electrical Conductivity (µS/cm)	^{222}Rn (Bq/L)	$\delta^{18}O$ (‰)	$\delta^{2}H$ (‰)
LS1	9.6	8.40	316	0.12	-18.5	-147.79
LS2	11.0	8.61	307	0.17	-18.4	-146.56
LS3	9.1	8.80	314	0.21	-18.3	-146.65
LS4	8.6	8.53	327	0.11	-18.3	-147.34
LS5	9.8	8.55	326	0.08	-18.1	-144.93
LS6	10.6	8.57	324	0.12	-18.1	-145.54
LS7	13.0	8.58	325	0.05	-17.9	-145.08
LS8	12.1	8.50	356	0.05	-17.4	-142.50
S1	7.0	8.58	345	0.08	-18.5	-146.69
S2	7.1	8.45	337	0.24	-18.6	-147.89
S3	8.8	8.50	393	0.31	-18.7	-147.75
S4	11.2	8.57	397	0.23	-18.6	-147.15
B1	9.7	8.38	442	0.21	-19.3	-151.42
B2	10.2	8.47	441	0.17	-19.2	-151.98
B3	10.1	8.35	446	0.29	-19.1	-151.04
B4	10.6	8.48	420	0.22	-19.1	-151.77
B5	12.0	8.50	415	0.32	-19.1	-150.91
B6	12.4	8.41	411	0.06	-19.0	-150.38
GIC 9486143	5.0	6.97	688	7.62	-19.2	-151.58
GIC 9486142	4.3	7.13	702	10.46	-19.8	-152.58
GIC 9486162	5.0	7.10	834	25.06	-20.2	-157.67
GIC 2096628	36.0	-	-	-	-12.3	-118.00

Abbreviations: Bq, becquerel; S, siemens.

Table 9. Water chemistry of river and groundwater samples – part 1, Fox Creek area, west-central Alberta.

Sample ID	pH	EC (µS/cm)	Ca (mg/L)	Mg (mg/L)	Na (mg/L)	K (mg/L)	Fe (mg/L)	Mn (mg/L)	Cl (mg/L)
LS1	8.26	295	44	10.4	4.9	0.6	0.03	<0.005	0.4
LS2	8.29	290	43.2	10.2	5.3	0.7	0.02	<0.005	<0.4
LS3	8.26	300	43.6	10.2	7.1	0.7	0.02	<0.005	0.4
LS4	8.28	309	43.6	10.1	8.4	0.7	0.02	<0.005	0.4
LS5	8.3	309	43.6	10.2	8.6	0.7	0.02	<0.005	0.4
LS6	8.33	309	43.7	10.1	8.8	0.7	0.01	<0.005	0.5
LS7	8.36	312	43.7	10.2	9.7	0.7	<0.01	<0.005	0.6
LS8	8.35	339	45.5	10.6	14.9	0.9	0.01	<0.005	1.1
S1	8.26	330	48	9.2	11.6	0.9	0.04	<0.005	0.4
S2	8.27	318	47.2	8.1	11.6	0.9	0.04	<0.005	0.5
S3	8.32	380	57.6	10.9	12	1	<0.01	<0.005	0.8
S4	8.38	381	57.2	11	13.1	1.1	<0.01	<0.005	0.6
B1	8.28	421	59.5	17.2	5.9	0.7	0.01	<0.005	0.7
B2	8.3	421	58.6	16.9	6	0.7	<0.01	<0.005	0.6
B3	8.3	417	56.5	16.4	6	0.7	0.02	<0.005	0.7
B4	8.32	395	58.1	15.7	6.5	0.8	0.02	<0.005	0.6
B5	8.34	394	56.7	15.6	6.4	0.7	<0.01	<0.005	0.6
B6	8.34	390	55.6	15.5	6.5	0.7	0.02	<0.005	0.6
GIC 9486143	7.37	729	86.2	24.1	12.5	1.78	0.906	-	7.37
GIC 9486142	7.55	743	54.7	13.9	80.2	1.80	0.822	-	7.55
GIC 9486162	7.43	889	64.9	12.4	114	5.12	0.952	-	7.43
GIC 2096628	8.23	3110	6.1	0.6	693	3.2	<0.02	0.01	8.23

Abbreviations: EC, electrical conductivity; S, siemens.

Table 10. Water chemistry of river and groundwater samples – part 2, Fox Creek area, west-central Alberta.

Sample ID	SO_4 (mg/L)	Carbonate (mg/L)	Bicarbonate (mg/L)	P-Alkalinity (mg/L as $CaCO_3$)	T-Alkalinity (mg/L as $CaCO_3$)	TDS (mg/L)	Hardness
LS1	2.5	<6	207	<5	170	165	153
LS2	2.5	<6	202	<5	165	161	150
LS3	3.1	<6	212	<5	174	169	151
LS4	3.5	<6	215	<5	176	172	151
LS5	3.6	<6	211	<5	173	171	151
LS6	3.8	<6	215	<5	176	173	151
LS7	4.3	<6	218	<5	179	177	151
LS8	6.8	<6	229	<5	187	192	157
S1	5.4	<6	232	<5	190	189	158
S2	4.9	<6	217	<5	178	180	151
S3	6.7	<6	266	<5	219	220	189
S4	8	<6	260	<5	214	219	188
B1	45.1	<6	242	<5	199	248	220
B2	43.5	<6	232	<5	190	241	216
B3	43.6	<6	235	<5	193	240	209
B4	32.2	<6	244	<5	200	234	210
B5	33	<6	234	<5	192	228	206
B6	32.2	<6	238	<5	195	228	202
GIC 9486143	21	<1	462	<1	378	378	314
GIC 9486142	37	<1	449	<1	368	412	194
GIC 9486162	28	<1	563	<1	462	506	213
GIC 2096628	15	<6	756	<5	620	1740	18

The following were below detection for all samples: Nitrate-N (<0.01 mg/L), Nitrite-N (<0.005 mg/L), Nitrate+Nitrite-N (<0.01 mg/L).
Abbreviation: TDS, total dissolved solids.

Table 11. Tritium, sulphur hexafluoride, and radiocarbon measurements for river and groundwater samples, Fox Creek area, west-central Alberta.

Sample ID	^{3}H (TU)	SF_6 (pptv; corrected for excess air)	SF_6 (fmol/kg)	SF_6 (pg/kg)	^{14}C (pMC)
LS1	7.85	6.331	2.436	0.342	79.43
LS2	7.69	6.759	2.461	0.365	81.46
LS3	7.82	6.750	2.669	0.364	81.71
LS4	7.21	6.449	2.607	0.348	-
LS5	7.25	6.633	2.472	0.358	82.08
LS6	7.43	6.800	2.534	0.367	82.16
LS7	7.59	7.723	2.616	0.417	82.54
LS8	7.60	6.648	2.336	0.359	81.67
S1	6.70	7.057	3.044	0.381	-
S2	7.03	7.413	3.190	0.400	79.98
S3	7.15	7.771	3.118	0.419	82.98
S4	7.35	6.765	2.464	0.365	83.4
B1	8.32	6.717	2.569	0.363	80.18
B2	8.49	6.532	2.450	0.353	81.05
B3	8.56	6.514	2.455	0.352	80.41
B4	8.44	7.401	2.736	0.399	80.54
B5	8.73	7.173	2.509	0.387	81.15
B6	8.95	6.935	2.390	0.374	81.66
GIC 9486143	4.52	1.353	0.864	0.073	-
GIC 9486142	1.07	0.186	0.141	0.010	-
GIC 9486162	0.11	0.126	0.091	0.007	-
GIC 2096628	0.05	-	-	-	0.9

Abbreviations: fmol, femtomoles; pg, picograms; pMC, percent of modern carbon; pptv, parts per trillion volume; TU, tritium units.

Table 12. Noble gas concentrations of river and groundwater samples, Fox Creek area, west-central Alberta.

Sample ID	Ar total (ccSTP/g)	Ne total (ccSTP/g)	Kr total (ccSTP/g)	Xe total (ccSTP/g)	He^4 (ccSTP/g)	R/Ra
LS1	3.82×10^{-4}	1.78×10^{-7}	9.34×10^{-8}	1.30×10^{-8}	4.08×10^{-8}	0.997
LS2	3.53×10^{-4}	1.78×10^{-7}	8.90×10^{-8}	1.29×10^{-8}	4.13×10^{-8}	0.987
LS3	3.82×10^{-4}	1.85×10^{-7}	9.50×10^{-8}	1.35×10^{-8}	4.19×10^{-8}	0.975
LS4	3.83×10^{-4}	1.82×10^{-7}	9.62×10^{-8}	1.40×10^{-8}	4.28×10^{-8}	0.993
LS5	3.75×10^{-4}	1.86×10^{-7}	9.14×10^{-8}	1.33×10^{-8}	4.30×10^{-8}	0.976
LS6	3.86×10^{-4}	1.83×10^{-7}	9.03×10^{-8}	1.28×10^{-8}	4.23×10^{-8}	0.989
LS7	3.69×10^{-4}	1.83×10^{-7}	9.12×10^{-8}	1.31×10^{-8}	4.25×10^{-8}	0.971
LS8	3.82×10^{-4}	1.82×10^{-7}	9.15×10^{-8}	1.30×10^{-8}	4.22×10^{-8}	0.976
S1	3.95×10^{-4}	1.84×10^{-7}	9.85×10^{-8}	1.49×10^{-8}	4.14×10^{-8}	0.975
S2	3.73×10^{-4}	1.83×10^{-7}	9.92×10^{-8}	1.42×10^{-8}	4.18×10^{-8}	0.963
S3	3.86×10^{-4}	1.97×10^{-7}	1.02×10^{-7}	1.45×10^{-8}	4.53×10^{-8}	0.974
S4	3.78×10^{-4}	1.83×10^{-7}	9.01×10^{-8}	1.32×10^{-8}	4.29×10^{-8}	0.988
B1	3.38×10^{-4}	1.72×10^{-7}	8.92×10^{-8}	1.20×10^{-8}	4.09×10^{-8}	0.964
B2	3.64×10^{-4}	1.71×10^{-7}	8.25×10^{-8}	1.23×10^{-8}	4.01×10^{-8}	0.988
B3	3.54×10^{-4}	1.76×10^{-7}	8.44×10^{-8}	1.17×10^{-8}	4.11×10^{-8}	0.976
B4	3.67×10^{-4}	1.72×10^{-7}	8.62×10^{-8}	1.23×10^{-8}	4.03×10^{-8}	0.997
B5	3.58×10^{-4}	1.81×10^{-7}	8.76×10^{-8}	1.16×10^{-8}	4.14×10^{-8}	0.984
B6	3.74×10^{-4}	1.78×10^{-7}	8.53×10^{-8}	1.23×10^{-8}	4.13×10^{-8}	0.991
GIC 9486143	5.08×10^{-4}	2.83×10^{-7}	1.20×10^{-7}	1.78×10^{-8}	6.15×10^{-8}	1.364
GIC 9486142	5.37×10^{-4}	3.23×10^{-7}	1.24×10^{-7}	1.86×10^{-8}	2.04×10^{-7}	0.380
GIC 9486162	5.66×10^{-4}	3.12×10^{-7}	1.29×10^{-7}	1.98×10^{-8}	6.37×10^{-8}	1.017
GIC 2096628	1.34×10^{-4}	2.13×10^{-7}	1.85×10^{-8}	1.82×10^{-9}	1.77×10^{-6}	0.036

Abbreviations: ccSTP, cubic centimetres at standard temperature and pressure; R/Ra, helium isotopic ratios.